Mineralogical Magazine, April 2001, Vol. 65(2), pp. 193–219

Computational methods for the study of energies of cation distributions: applications to cation-ordering phase transitions and solid solutions

A. BOSENICK[1,2], M. T. DOVE[1,*,†], E. R. MYERS[1,3], E. J. PALIN[1], C. I. SAINZ-DIAZ[4], B. S. GUITON[1], M. C. WARREN[1,5], M. S. CRAIG[1] AND S. A. T. REDFERN[1]

[1] Department of Earth Sciences, University of Cambridge, Downing Street, Cambridge CB2 3EQ, UK
[2] Present address: Martenshofweg 9, 24109 Kiel, Germany
[3] Present address: Department of Pure Mathematics and Mathematical Statistics, University of Cambridge, 16 Mill Lane, Cambridge CB2 1SB, UK
[4] Estacion Experimental del Zaidin, CSIC, C/ Profesor Albareda, 1, 18008-Granada, Spain
[5] Present address: Department of Earth Sciences, The University of Manchester, Manchester M13 9PL, UK

ABSTRACT

The structural and thermodynamic properties of minerals are strongly affected by cation site-ordering processes. We describe methods to determine the main interatomic interactions that drive the ordering process, which are based on parameterizing model Hamiltonians using empirical interatomic potentials and/or *ab initio* quantum mechanics methods. The methods are illustrated by a number of case study examples, including Al/Si ordering in aluminosilicates, Mg/Ca ordering in garnets, simultaneous Al/Si and Mg/Al ordering in pyroxenes, micas and amphiboles, and Mg/Al non-convergent ordering in spinel using only quantum mechanical methods.

KEYWORDS: Monte Carlo simulation, cation ordering, interatomic potentials, phase transitions, aluminosilicates.

Introduction

THIS paper gives a review of computational methods that can be used to calculate the energies associated with the site ordering of cations in minerals. The discussion encompasses a wide range of phenomena, including cation-ordering phase transitions (such as Al/Si ordering on tetrahedral sites in aluminosilicates) and solid solutions in which there are no phase transitions (Putnis, 1992). The central point is that both short-range and long-range structural ordering are driven by short-range energies. In the simplest cases these can be represented by simple bond energies, but this is not a necessary limitation.

* E-mail: martin@esc.cam.ac.uk
† Corresponding author

The approach we discuss here is based on models for calculating the energies of different atomic configurations of a given material. Often these energies are represented by simple empirical functions with parameters that are tuned against experimental data. But empirical models have their limitations, so we need also to consider the possible use of quantum mechanics methods.

In this paper we will review the basic approach that has been developed in Cambridge for the determination of energies of ordering of cations in minerals (e.g. Thayaparam *et al.*, 1994, 1996; Bosenick *et al.*, 2000; Dove *et al.*, 2000). We first describe the models that are used to describe the interactions between atoms, based either on empirical functions or quantum mechanics methods. Secondly, we outline how the ordering energies can be described in terms of individual bond energies, thus allowing the total bond energy of a system to be reduced to a small number of

parameters. We explain how, in principle, these parameters can be obtained from appropriate calculations. Thirdly we describe the practical approach to determining these problems based on the use of spreadsheet calculations. Finally, we present a number of examples that illustrate various aspects of the calculations outlined in this paper.

The motivation for this work is the need to determine a set of interaction parameters for statistical mechanics applications. Our own objective is to use these interactions in Monte Carlo simulations of ordering processes (e.g. Thayaparam *et al.*, 1994, 1996; Myers *et al.*, 1998; Dove, 1999; Dove *et al.*, 2000), as described in the following paper (Warren *et al.*, 2001). However, the interactions can also be used in other statistical mechanics tools such as the Cluster Variation Method, as recently applied to studies of Al/Si ordering in aluminosilicates (Vinograd and Putnis, 1999, Vinograd *et al.*, 2001) and to Zn-Fe mixing in sulphides (Balabin and Sack, 2000). Moreover, taken by themselves, the relative sizes of exchange interactions may provide fairly immediate insights into the driving mechanisms of ordering processes (examples are given below). Our approach is dominated by the application to cation ordering in mineral systems, such as (but not exclusively) Al/Si ordering on tetrahedral sites and Mg/Al ordering in octahedral sites in aluminosilicates. We have found that the approach described here works well for such examples, probably because the ordering energies are primarily associated with localized structure relaxations associated with strain interactions of 'reasonable' size. We have tried adapting these methods to the study of oxygen-vacancy ordering in perovskites, but were unsuccessful. This possibly represents the hardest case one might wish to study, because the formation of a vacancy is always associated with a significant displacement of the cation in the polyhedron from which the oxygen atom is removed. However, it does alert us to the fact that there is a limit to the range of situations to which our methods can be applied, although we note that oxygen vacancy ordering in alumina has been studied using a similar approach (Lee *et al.*, 1997).

Models for the interatomic interactions

Models based on parameterized empirical functions

The essential component of the approach is a method to calculate the energies between atoms. In the formalism we will present later, we will represent the energy associated with the ordering of atoms in terms of the energies of individual bonds (pair interactions), but this does not require us to use only pair potentials in the initial calculations. For silicates we use empirical models based on the shell model devised for silica by Sanders *et al.* (1984). Short-range interactions are modelled using Buckingham potentials:

$$\varphi(r) = B\exp(-r/\rho) - Cr^{-6}$$

The first term is the 'repulsive interaction', which arises from overlap of electrons on neighbouring atoms. Its functional form appears to be a good representation of quantum mechanics calculations (Post and Burnham, 1986). The second term is the 'dispersive interaction', which is due to correlated fluctuations in the electron densities of pairs of atoms. It is most appropriate for polarizable ions such as O^{2-}, but it is used in the model for the Si....O bond as a means of providing additional parameterization.

Covalent effects are modelled by use of harmonic potentials that depend on the O—Si—O angle θ:

$$\varphi(\theta) = \tfrac{1}{2}k(\theta - \theta_0)^2$$

This potential acts to provide a force against deformation of the SiO_4 tetrahedra, a role that would otherwise have to be played by the O...O potentials. The potential is also used for the O—Al—O bond angle in aluminosilicates.

Long-range Coulomb interactions are treated using formal charges, because this makes transferability rather easier to build into the models. It appears that the use of formal charges has no significant effect when modelling the structures and lattice dynamics of aluminosilicates (Winkler *et al.*, 1991; Patel *et al.*, 1991; Sainz-Diaz *et al.*, 2001). However, quantum mechanics tests of Al/Si tetrahedral ordering energies suggest that formal charges provide a slight overestimation of the energy required to replace two Al—O—Si linkages by the pair Si—O—Si and Al—O—Al (McConnell *et al.*, 1997).

Electronic polarizability is treated by using a shell model for the oxygen anion, in which there is an harmonic energy associated with the displacement, d, of the centre of the positively charged core with respect to the centre of the shell:

$$\varphi(d) = \tfrac{1}{2}Kd^2$$

Parameters for interactions involving silicon and oxygen were fitted to experimental data for quartz. Parameters for other cations are taken from other empirical studies or from electron gas quantum mechanics calculations (Post and Burnham, 1986). The models have been tested in some detail for a wide range of aluminosilicate minerals (Winkler *et al.*, 1991; Patel *et al.*, 1991; Sainz-Diaz *et al.*, 2001), enabling them to be used for a wide range of aluminosilicates with some confidence.

Calculations with empirical functions were performed with the GULP lattice energy code (Gale, 1997). This adjusts the atomic coordinates and unit-cell parameters to minimize the lattice energy. When the positions of two cations are exchanged, there is necessarily some relaxation of the atomic positions, because exchanging the positions of two cations of different sizes leads to changes in local forces. These forces will be relieved by the energy-minimization process.

Empirical models are surprisingly good (Winkler *et al.*, 1991), particularly when it is appreciated that in many cases the parameterization has not taken account of energies. Instead, the models are usually parameterized against crystal structures and physical properties, which depend on the derivatives of the interatomic potentials but not on the actual values. Our experience is that for many cases the empirical models give reasonable values for the ordering energies, but there are cases when empirical models would be inappropriate. These include cases when atoms jump between sites of different coordination. An example is the ordering of Mg and Al cations between the tetrahedral and octahedral sites in spinel (Warren *et al.*, 2000*a,b*). In such cases there is a change in energy associated with a cation moving from one type of site to another, and it is unlikely that this energy will be properly represented by the empirical models. For these applications, the only viable approach is the use of quantum mechanics calculations.

Models based on quantum mechanics electronic structure calculations

Our approach in using quantum mechanics methods is to use the 'Density Functional Theory' (DFT) implementation of many-electron quantum mechanics (Payne *et al.*, 1992). The main approximation in this approach is in the way the exchange and correlation energies are treated, because there is no explicit formulation of these energies. We use one of two standard methods, the 'local density approximation' (LDA) and the 'generalized gradient approximation' (GGA). Neither approach is perfect, and there are cases when either may give better results than the other, although it is hoped that any differences will not be large. Electronic structure calculations are made easier by using the pseudopotential method to represent the inner electrons in atoms, which means that we only need to explicitly consider the wave functions of the outer electrons in each atom.

We initially used the most common implementation of DFT for the study of solids, which is based on the use of the superposition of plane waves to represent the electronic wave functions. A number of codes are available, many of which have been developed for parallel computers; we used the CASTEP/CETEP programs (CASTEP 4.2 Academic version, licensed under the UKCP-MSI® Agreement, 1999; Payne *et al.*, 1992; Clarke *et al.*, 1992). The amplitudes of the plane waves are varied to lower the total energy in line with the variational principle. Plane waves are particularly appropriate when there is an inherent periodicity in the system being studied. One of the advantages of the plane-wave approach is that there are no restrictions on the form of the electron distribution, and any deficiencies in the calculations will arise from the use of the LDA or GGA approximations or the use of the pseudopotential method. The main disadvantage of the plane-wave approach is that the size of the calculation scales as the size of the system, N, with a power-law dependence of between N^2 and N^3. As a result, the study of large systems is problematic, and the potential contribution of the quantum mechanics methods is limited as a result.

Methods for which the size of the calculation is able to scale more-or-less linearly with system size, known as 'Order-N' or '$O(N)$' methods, are based on a real-space description of the electron density. We have been using the SIESTA code (Ordejón *et al.*, 1996; Artacho *et al.*, 1999), which uses atom-centred electron orbitals, similar to those familiar in quantum chemistry, to represent the electron density within the formalism of DFT (with either the LDA or GGA implementations of the exchange and correlation energies). SIESTA also uses the pseudopotential method. We have shown that the use of SIESTA can give reasonable results for a wide range of aluminosilicate minerals (Craig *et al.*, 2001), although for calculations of ordering energies we have found

that SIESTA does not give as high an accuracy as the plane-wave methods because it is harder to form a near-complete basis set for an atom-centred basis than with plane waves. However, because it is possible to perform more calculations on complex systems, SIESTA is able to play an important role when quantum mechanics methods are needed to overcome some deficiencies of empirical methods. Moreover, it is likely that new developments in the use of atomic orbitals will allow this approach to become more accurate. At the present time, our experience is that for highly accurate calculations, so many orbitals may be needed that some of the advantages over plane wave methods are lessened.

We should remark that in some cases the issue is not of whether to choose between empirical models or quantum mechanics, but instead a combination can be used. Quantum mechanics methods can be used to tune empirical models or to fill in for some deficiencies of the empirical models. As we have noted above, quantum mechanics methods are essential when calculating the energy associated with a cation moving between different types of sites (what we will call the 'chemical potential' below). We have found, however, that empirical models are able to give reasonable results for the changes in bond energies associated with cations exchanging positions between similar types of sites (what we will call the 'exchange interaction' below). The methods used to compute these energies involve a large number of calculations of the energies of different atomic configurations, as will be described below. The number of configurations is usually too large for quantum mechanics methods to be practical. But it is possible to perform these calculations with empirical methods, and to check some specific configurations with quantum mechanics methods in order to tune the empirical energies. This was an approach used to test the energies associated with Al/Si ordering in tetrahedral sites in aluminosilicates (McConnell *et al.*, 1997) as mentioned above. Another approach is to use the bond energies obtained by empirical models, and to use the quantum mechanics calculations to obtain the energies associated with atoms moving between different types of sites. The proviso on this is that there should not be a strong correlation between the fitted values of this energy and the exchange energies, as discussed below.

Basic theory

The initial approach is to represent the energy of a system in terms of individual bonds (Putnis, 1992; Dove, 1999; Dove *et al.*, 2000). For example, if we have a simple network containing atoms of type **A** and **B**, for a given bond type we assume that the energy can be expressed in terms of the separate **A–A**, **A–B** and **B–B** bond energies:

$$E = N_{\mathbf{AA}}E_{\mathbf{AA}} + N_{\mathbf{BB}}E_{\mathbf{BB}} + N_{\mathbf{AB}}E_{\mathbf{AB}}$$

where $N_{\mathbf{AA}}$ etc. are the numbers of each type of bond, and $E_{\mathbf{AA}}$ etc. are the energies of each type of bond. Clearly the sum of the different types of bonds must be equal to the total number of bonds, which implies that there must be some interdependence between the numbers of different bond types (e.g. both $N_{\mathbf{AB}}$ and $N_{\mathbf{BB}}$ are determined by $N_{\mathbf{AA}}$, as demonstrated below). In fact, for many cases the numbers of each type of bond depend on the number of only one type. In what follows we show for a few special cases how the number of independent variables can be reduced in this way. We chose our examples to show how to make this reduction, but we also present a small number of counter examples to show that one has to be careful about over-generalizing. Our set of examples is not exhaustive of all the types of cases one might encounter, but it should be possible to adapt the principles to any new case.

Although most of our analysis is in terms of the pair energies defined above, it is possible that there will be energy terms that depend on the distribution of larger groups of atoms. In our work on mineral systems we have generally found that the use of such terms does not significantly improve the quality of the model representation of the ordering energy, since the effects can usually be taken into account by the use of a larger set of pair interactions. For the case of spinel (discussed later), a multi-site energy term was included in order to reduce the number of independent pair energy terms, but in other cases the use of a consistent set of multi-site terms is likely to increase the number of energy terms.

We note at the outset that for simulations of solid solutions we do not assume that the energies $E_{\mathbf{AA}}$ etc. are independent of the chemical composition. However, we have found for several example systems that the ordering energies are more-or-less independent of the chemical composition provided that it is only the compositions of the ordering cations that change. For the case where there are two ordering

cations, this insensitivity to composition has the effect that the formalism is symmetric in composition about 50:50 mixtures.

Case I: A network of sites with fixed numbers of **A** *and* **B** *cations*

We first consider the simplest case of a single network of N symmetrically equivalent sites, as illustrated in Fig. 1. This case has a fraction x of **A** atoms and fraction $(1 - x)$ of **B** atoms. Each site has z neighbours. We take the number of **A**—**A** bonds, which we label $N_{\mathbf{AA}}$, as the fundamental variable. For each **A** atom, the probability that a given neighbour is also an **A** atom is written as $P_{\mathbf{AA}}$. The number of **A**—**A** bonds follows from the product of the number of **A** atoms and the probability of each of these having an **A** atom as a neighbour in each bond:

$$N_{\mathbf{AA}} = \tfrac{1}{2}\, zNxP_{\mathbf{AA}}$$

The factor of Ý is included to avoid counting each bond twice. The number of **A**—**B** bonds is simply given by product of the number of **A** atoms and the probability that each bond has a **B** neighbour:

$$N_{\mathbf{AB}} = zxN(1 - P_{\mathbf{AA}}) = zxN - 2N_{\mathbf{AA}}$$

Finally, the number of **B**—**B** bonds is equal to the total number of bonds minus the number of **A**—**A** and **A**—**B** bonds:

$$\begin{aligned} N_{\mathbf{BB}} &= \tfrac{1}{2}\, zN - N_{\mathbf{AA}} - N_{\mathbf{AB}} \\ &= \tfrac{1}{2}\, zN(1 - 2x) + N_{\mathbf{AA}} \end{aligned}$$

We recall from above that if the energy to form an **A**—**A** bond can be written as $E_{\mathbf{AA}}$, and likewise for $E_{\mathbf{AB}}$ and $E_{\mathbf{BB}}$, the total energy can be written as:

$$\begin{aligned} E &= N_{\mathbf{AA}}E_{\mathbf{AA}} + N_{\mathbf{BB}}E_{\mathbf{BB}} + N_{\mathbf{AB}}E_{\mathbf{AB}} \\ &= N_{\mathbf{AA}}E_{\mathbf{AA}} + \left(\tfrac{1}{2}zN(1 - 2x) + N_{\mathbf{AA}}\right)E_{\mathbf{BB}} + \\ &\qquad (zxN - 2N_{\mathbf{AA}})E_{\mathbf{AB}} \\ &= N_{\mathbf{AA}}(E_{\mathbf{AA}} + E_{\mathbf{BB}} - 2E_{\mathbf{AB}}) + \\ &\qquad \tfrac{1}{2}\, zN(2xE_{\mathbf{AB}} + (1 - 2x)E_{\mathbf{BB}}) \\ &= N_{\mathbf{AA}}J + E_0 \end{aligned}$$

E_0 is the constant term that does not depend on the number of bonds of any specific type, and J is the energy associated with atoms exchanging positions so as to replace two **A**—**B** bonds with an **A**—**A** and a **B**—**B** bond. J is called the 'exchange interaction', and is of central importance in the process of modelling cation ordering. A positive value of J implies that it is energetically preferable for the two sites to contain different cations, whereas a negative value implies that it is energetically preferable for the two sites to contain the same cations. The example we have worked through shows that the total energy can be written in terms of the number of **A**—**A** bonds only, the point being that the numbers of **A**—**B** and **B**—**B** bonds are completely determined by the number of **A**—**A** bonds. The formation of an **A**—**A** bond implies the formation also of a **B**—**B** bond and the loss of two **A**—**B** bonds. This is a common feature, and is exploited in the methods developed to determine values of the exchange interaction J. Incidentally, one could therefore argue that Löwenstein's rule of Al—Al avoidance in framework aluminosilicates is also a rule of Si—Si avoidance.

We note for future reference that it follows from this analysis that we cannot determine the values of $E_{\mathbf{AA}}$, $E_{\mathbf{BB}}$ or $E_{\mathbf{AB}}$ separately. Because of the constraints on the numbers of atom pairs, which we exploited to reduce the number of interactions to just J and E_0, we do not have independent equations to allow the separate bond energies to be extracted from a system with a fixed composition. In principle, it might be thought that these could be extracted if simulations can be run at several different compositions through the dependence of E_0 on the composition, assuming that there is not a dependence of J on composition through a non-analytical process (indeed, we often find that J is independent of composition). However, there will be an intrinsic dependence of E_0 on composition, which arises from the normal chemical potential not considered in this analysis.

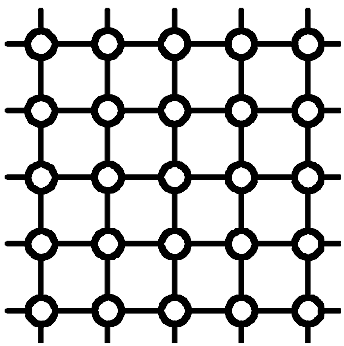

FIG. 1. Representation of a network.

The picture given here also applies in the case where there the network is not fully linked, as illustrated in Fig. 2. In these examples, we have chains of sites, or pairs of sites. When the equations are written for this case, the same result is obtained as for the fully linked network, even when allowing the composition of each set of linked sites to vary.

Case 2: A network of sites with variable numbers of **A** *and* **B** *cations*

The case where the numbers of **A** and **B** cations are variable represents the case where there are several different types of sites. An example might be two networks between which cations can be exchanged, for which we need to define the interactions between the atoms of a single network (Fig. 3). In this case we cannot simply reduce everything to just the count of one type of bond. Instead, we write the number of **A**–**B** bonds in terms of the number of **A**–**A** and **B**–**B** bonds:

$$N_{\mathbf{AB}} = \tfrac{1}{2} zN - N_{\mathbf{AA}} - N_{\mathbf{BB}}$$

Thus the total bond energy can be written as

$$\begin{aligned} E &= N_{\mathbf{AA}}E_{\mathbf{AA}} + \\ &\quad N_{\mathbf{BB}}E_{\mathbf{BB}} + \left(\tfrac{1}{2}zN - N_{\mathbf{AA}} - N_{\mathbf{BB}}\right) E_{\mathbf{AB}} \\ &= N_{\mathbf{AA}}(E_{\mathbf{AA}} - E_{\mathbf{AB}}) + N_{\mathbf{BB}}(E_{\mathbf{BB}} - E_{\mathbf{AB}}) + \tfrac{1}{2} zNE_{\mathbf{AB}} \end{aligned}$$

In this formulation, the energy is now a function of both $N_{\mathbf{AA}}$ and $N_{\mathbf{BB}}$. Alternatively, noting from above that if a particular configuration of the network contains a fraction x of **A** atoms,

$$N_{\mathbf{BB}} = \tfrac{1}{2} zN(1 - 2x) + N_{\mathbf{AA}}$$

we can rewrite the energy as

$$\begin{aligned} E &= N_{\mathbf{AA}}(E_{\mathbf{AA}} - E_{\mathbf{AB}}) + \\ &\quad \left(\tfrac{1}{2}zN(1-2x) + N_{\mathbf{AA}}\right)(E_{\mathbf{BB}} - E_{\mathbf{AB}}) + \tfrac{1}{2} zNE_{\mathbf{AB}} \\ &= N_{\mathbf{AA}}(E_{\mathbf{AA}} + E_{\mathbf{BB}} - 2E_{\mathbf{AB}}) - \\ &\quad zNx(E_{\mathbf{BB}} - E_{\mathbf{AB}}) + \tfrac{1}{2} zNE_{\mathbf{BB}} \\ &= N_{\mathbf{AA}}J - \mu Nx + E_0 \end{aligned}$$

This is identical to the equation in the first case discussed, but now we explicitly take account of the term that depends on x, which is to be treated as a variable. This new term has the form of a chemical potential, as represented by the constant μ:

$$\mu = z(E_{\mathbf{BB}} - E_{\mathbf{AB}})$$

It should be noted that the variation in composition in one network will give rise to a corresponding variation in composition on the second (or other) network(s). The expression for the bond energies on the other networks will give rise to new chemical potential terms. However, it is likely that the different networks correspond to sites of different symmetry. It may even be the case (as we will find in the example of spinel later) that the different sites have different coordination number. Therefore, it is likely that there will also be an intrinsic energy of moving an atom from one type of site to another, independent of the changes in the bond energies we have been discussing. These energies can also be expressed as chemical potentials, and we can

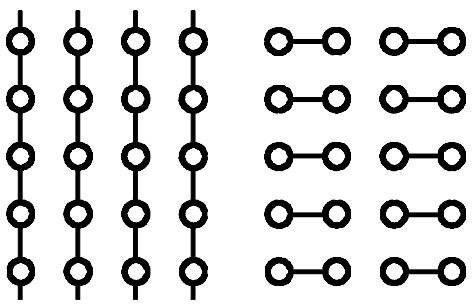

FIG. 2. Examples of networks of sites that are not linked.

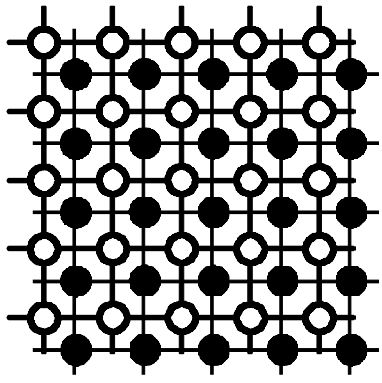

FIG. 3. Two networks between which cations can be exchanged.

subsume the bond contributions and the intrinsic site energies into a single chemical potential.

It is important to realise that there are constraints operating on the chemical potentials. For example, we have shown that if, for one type of site, there is a fraction x of one type of atom and $1-x$ of the other type, the chemical potential can be reduced to a single function of x. Now suppose that we have n types of sites, and two types of atoms, **A** and **B**. For each type of site, which we label by i, we have a fraction x_i of atom type **A**, and a corresponding chemical potential μ_i. We now have the constraint that

$$\sum_{i=1}^{n} x_i = 1 \Rightarrow x_n = 1 - \sum_{i=1}^{n-1} x_i$$

The chemical potential energy can therefore be written as

$$E_\mu = \sum_{i=1}^{n} \mu_i x_i = \mu_n + \sum_{i=1}^{n-1} (\mu_i - \mu_n) x_i = E_0 + \sum_{i=1}^{n-1} \bar{\mu} x_i$$

We conclude that for n sites, there will be $n-1$ independent chemical potential terms. Although each term is a mixture of bond and site energies, it will be sufficient to treat all effects together in the set of values of μ_i.

Case 3: Interactions between two distinct networks of sites with **A** *and* **B** *cations in one network and* **A** *and* **C** *cations in the second network*

The case with two distinct networks is illustrated in Fig. 4. Here we are interested in the interactions *between* networks, represented by the vertical bonds. We consider the case where there are N atoms in each network, with a mixture of xN **A** and $(1-x)N$ **B** cations on one network, and a mix of yN **A** and $(1-y)N$ **C** cations on the second network. The number of **A—A** bonds *between* the networks is denoted as $N_{\mathbf{AA}}$. Thus the number of **A—C** bonds *between* the networks is

$$N_{\mathbf{AC}} = xN - N_{\mathbf{AA}}$$

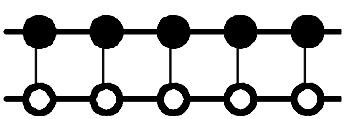

FIG. 4. Two distinct networks.

The number of **B—A** bonds *between* the networks is

$$N_{\mathbf{BA}} = yN - N_{\mathbf{AA}}$$

Finally, the number of **B—C** bonds *between* the networks is

$$N_{\mathbf{BC}} = N - N_{\mathbf{AA}} - N_{\mathbf{AC}} - N_{\mathbf{BA}} = (1 - x - y)N + N_{\mathbf{AA}}$$

Thus the bond energy is equal to

$$\begin{aligned} E &= N_{\mathbf{AA}}E_{\mathbf{AA}} + E_{\mathbf{AC}}(xN - N_{\mathbf{AA}}) + \\ &\quad E_{\mathbf{BA}}(yN - N_{\mathbf{AA}}) + E_{\mathbf{BC}}((1 - x - y)N + N_{\mathbf{AA}}) \\ &= N_{\mathbf{AA}}(E_{\mathbf{AA}} + E_{\mathbf{BC}} - E_{\mathbf{AC}} - E_{\mathbf{BA}}) + \\ &\quad N(xE_{\mathbf{AC}} + yE_{\mathbf{BA}}) + (1 - x - y)E_{\mathbf{BC}}) \\ &= N_{\mathbf{AA}}J_{\mathbf{AA}} + E_0 \end{aligned}$$

Again, this depends only on one number, which we have chosen to be $N_{\mathbf{AA}}$. Note, however, that J, which we have labelled $J_{\mathbf{AA}}$, is now defined in terms of the bond energies in a way that is different from the case where we had only two types of ordering atom. It is because the definition is not symmetric with respect to the atom types that we label it $J_{\mathbf{AA}}$ instead of just J as in the two-atom case. Similar definitions will be found in the general case (case 4 below) of a system with three ordering atoms.

Case 4: A network of sites with fixed numbers of **A**, **B** *and* **C** *cations*

The network we now describe is the same as in Case 1, but now we have three ordering cations instead of two. We consider the case of three ordering atoms, **A**, **B** and **C**, with proportions x, y and $1-x-y$ respectively, and a lattice with one type of site having z neighbours. We begin, as before, by considering the **A** atoms. Each site containing an **A** atom has the probability $P_{\mathbf{AA}}$ that a neighbouring site also contains an **A** atom. Thus, if there are N sites in total, we can write the number of **A—A** linkages as

$$N_{\mathbf{AA}} = \tfrac{1}{2} zNxP_{\mathbf{AA}}$$

Hence it follows that the number of **A—B** and **A—C** linkages is

$$N_{\mathbf{AB}} + N_{\mathbf{AC}} = zNx(1 - P_{\mathbf{AA}}) = zNx - 2N_{\mathbf{AA}}$$

Similar equations follow for other pairs of atom types, and it is easiest to express all the equations in matrix form:

$$\begin{pmatrix} 0 & 1 & 1 \\ 1 & 0 & 1 \\ 1 & 1 & 0 \end{pmatrix} \begin{pmatrix} N_{\mathbf{BC}} \\ N_{\mathbf{AC}} \\ N_{\mathbf{AB}} \end{pmatrix} = \begin{pmatrix} zNx - 2N_{\mathbf{AA}} \\ zNy - 2N_{\mathbf{BB}} \\ zN(1-x-y) - 2N_{\mathbf{CC}} \end{pmatrix}$$

The solutions of this matrix equation are

$$N_{\mathbf{BC}} = zN(1 - 2x)/2 + (N_{\mathbf{AA}} - N_{\mathbf{BB}} - N_{\mathbf{CC}})$$
$$N_{\mathbf{AC}} = zN(1 - 2y)/2 + (N_{\mathbf{BB}} - N_{\mathbf{AA}} - N_{\mathbf{CC}})$$
$$N_{\mathbf{AB}} = zN(2x + 2y - 1)/2 + (N_{\mathbf{CC}} - N_{\mathbf{AA}} - N_{\mathbf{BB}})$$

The result is that the energy equations can be expressed in terms of the three variables $N_{\mathbf{AA}}$, $N_{\mathbf{BB}}$ and $N_{\mathbf{CC}}$. The energy can therefore be written as

$$\begin{aligned} E = {} & (E_{\mathbf{AA}} + E_{\mathbf{BC}} - E_{\mathbf{AB}} - E_{\mathbf{AC}})N_{\mathbf{AA}} + \\ & (E_{\mathbf{BB}} + E_{\mathbf{AC}} - E_{\mathbf{AB}} - E_{\mathbf{BC}})N_{\mathbf{BB}} + \\ & (E_{\mathbf{CC}} + E_{\mathbf{AB}} - E_{\mathbf{AC}} - E_{\mathbf{BC}})N_{\mathbf{CC}} + \\ & \tfrac{zN}{2}(E_{\mathbf{AB}}(2x + 2y - 1) + \\ & E_{\mathbf{AC}}(1 - 2y) + E_{\mathbf{BC}}(1 - 2x)) \\ = {} & J_{\mathbf{AA}}N_{\mathbf{AA}} + J_{\mathbf{BB}}N_{\mathbf{BB}} + J_{\mathbf{CC}}N_{\mathbf{CC}} + E_0 \end{aligned}$$

where the exchange constants and constant term are now defined as

$$\begin{aligned} J_{\mathbf{AA}} &= (E_{\mathbf{AA}} + E_{\mathbf{BC}} - E_{\mathbf{AB}} - E_{\mathbf{AC}} \\ J_{\mathbf{BB}} &= (E_{\mathbf{BB}} + E_{\mathbf{AC}} - E_{\mathbf{AB}} - E_{\mathbf{BC}}) \\ J_{\mathbf{CC}} &= (E_{\mathbf{CC}} + E_{\mathbf{AB}} - E_{\mathbf{AC}} - E_{\mathbf{BC}}) \\ E_0 &= \tfrac{zN}{2}\,(E_{\mathbf{AB}}(2x + 2y - 1) + E_{\mathbf{AC}}(1 - 2y) + \\ &\qquad E_{\mathbf{BC}}(1 - 2x)) \end{aligned}$$

Note that the definition of the exchange interactions has the same form as in case 3 above, where we also considered the presence of three types of ordering atoms (albeit with a particular separation across two networks).

The important difference between this result, where we now have three exchange constants, and that of the earlier results where there was only one exchange constant, is due to the different balance between the number of bond types and the number of constraints in the equations. In the case of the binary system, there were 3 variables, $N_{\mathbf{AA}}$, $N_{\mathbf{AB}}$ and $N_{\mathbf{BB}}$, and 2 *independent* constraints, namely the total number of atoms of type **A**, and the total number of bonds. The former ensured that the value of $N_{\mathbf{AB}}$ was linked to the value of $N_{\mathbf{AA}}$, and the second ensured that the value of $N_{\mathbf{BB}}$ was then tied to both $N_{\mathbf{AA}}$ and $N_{\mathbf{AB}}$. In the case of having three ordering atoms, there are six variables ($N_{\mathbf{AA}}$, $N_{\mathbf{BB}}$, $N_{\mathbf{CC}}$, $N_{\mathbf{AB}}$, $N_{\mathbf{AC}}$, $N_{\mathbf{BC}}$) and three constraints, namely the number of **A** and **B** atoms and the total number of bonds. The balance means that there will be three variables whose values are undetermined by the constraints, and in these equations we have chosen these to be the numbers of bonds between *like* atoms. Some comments on the implementation of this case will be discussed at the end of the next section.

This argument can be generalized to the case where there are n types of ordering atom. Then there will be $n(n+1)/2$ bond variables and n constraints, and hence $n(n-1)/2$ independent bond variables. Noting that with n types ordering atoms there will be n types of neighbours of like atoms and $n(n-1)/2$ types of neighbours with unlike atoms, it will then be preferable to recast the equations here to give the energies in terms of the numbers of bonds with unlike atoms. This is relatively straightforward following the discussion here. If we have any number of ordering atoms, each with proportion x_1, x_2, etc., subject to the sum of proportions equal to 1, the number of bonds involving the same atom (labelled i) is

$$N_{ii} = zNx_i - \sum_j N_{ij}$$

The set of N_{ii} can be substituted into the general energy equation

$$E = E_0 + \sum_{\langle ij \rangle} N_{ij}E_{ij}$$

where the angle brackets in the summation denote the fact that no bond should be counted twice. This substitution gives an energy expression that only contains terms where $i \neq j$.

Effects of temperature

The procedure outlined above has not taken account of temperature or pressure; it has been tacitly assumed that neither of these have significant effects. We have performed some tests with garnet to show that the ordering energies are not affected by pressure in this case, and our experience that constraining or relaxing the volume has little effect on the calculated ordering energies supports this specific test. We do not anticipate that temperature will have an effect, but this is much harder to evaluate because it would mean going beyond the static energy minimization method. We note that some tests along these lines are being carried out on simple systems by Allan and co-workers (Allan *et al.*, 2000).

Implementation

General principles

By expressing the energy in terms of the energies of specific bond types, we have provided a relatively simple representation of the energy. There will usually be several different types of bonds to consider, as represented by Fig. 5. In this picture, there are two different types of sites, and the sites are linked by interactions of different types as represented by the different thicknesses of the bonds. The energy of any configuration can be represented by the general expression

$$E = \sum_{\langle i,j \rangle} N_{\mathbf{AA}}^{\langle i,j \rangle} J_{ij} + \sum_{j} \mu_j x_{\mathbf{A}}^{j} + E_0$$

The first term sums over all types of bond (the angle brackets denote the sum is over pairs of atoms, avoiding double counting of bonds), and the second term sums over all types of sites. We now allow the exchange interactions J_{ij} to depend on the type of bond formed by the pair of sites i and j (e.g. nearest neighbour, second neighbour etc.), and allow the chemical potential μ_j to depend on the site if there is more than two types of distinct sites. The task is to obtain the complete set of exchange energies J_{ij} and the chemical potential energies μ_j.

Our approach is to produce a large number of configurations with different arrangements of atoms and to compute the energies of each configuration following the minimization of the lattice energy. Each configuration consists of a large unit cell that is a supercell of the unit cell of the system, and the periodic boundaries are retained to avoid effects of surfaces and finite sizes. The different cations are distributed across the cation sites at random. The lattice energy of each configuration is relaxed in order to relieve stresses associated with the exchange of cations of different sizes. After the energies of many configurations have been obtained, the values of the parameters J and μ are fitted against the database of energies (of course, the fitting procedure will also include E_0, but this quantity is of no subsequent interest in the study of ordering behaviour). We have found that between 50–100 configurations are useful for this procedure.

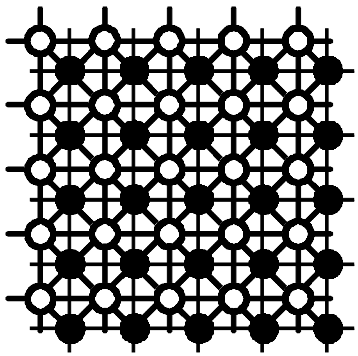

FIG. 5. Two different types of sites, linked by interactions of different types.

As an aside at this point, we remark that it is not clear whether, in principle, one should allow the unit-cell parameters to relax in the minimization of the energy of each configuration. One could argue that the relaxation of the unit cell allows for complete relaxation of the stresses and is therefore a good thing. On the other hand, one could also argue that the use of periodic boundary conditions simulates the embedding of a small region of the crystal within a disordered matrix, and that by allowing relaxation of the unit cell parameters also changes the density of the matrix. Fortunately, we have found that these questions of principle do not need to be resolved, because the energy changes associated with relaxation of the lattice parameters are not significant if an appropriate set of initial lattice parameters are chosen and if the supercell is large enough. Moreover, the computational effort required to obtain the energies of many configurations can be reduced if there is no need to relax the lattice stresses as well as the forces on the atoms. For calculations with empirical interatomic potentials, the initial lattice parameters can be obtained from a full lattice energy minimization using the 'virtual crystal approximation', in which the cation sites are treated as having partial occupancies of the different disordered cations with their interactions given by an appropriate average of those of the disordered cations. The virtual crystal approximation gives a reasonable reproduction of a disordered crystal (Winkler *et al.*, 1991; Dove and Redfern 1999; Sainz-Diaz *et al.*, 2001), unless one is aiming at accurate calculations of subtle effects such as excess volumes associated with solid solutions (Bosenick *et al.*, 2001). Such a scheme is being developed for quantum mechanical calculations.

Spreadsheet solution

The general approach lends itself to automation, and one of us (AB) has developed a spreadsheet implementation of the method. This is based on Microsoft Excel, but the principles can be applied within most other programming environments. The general procedure, which starts from the crystal structure and leads to the production of a file containing input data for a Monte Carlo simulation of the ordering processes, is sketched in Fig. 6.

The starting crystal structure is used to produce a supercell of appropriate size. Typically it is useful for the supercell to be of a size such that there is of the order of a few tens of sites over which ordering occurs, which we call the **X**-sites. Each of the N **X**-sites is initially occupied by two different cations, which we label as species **A** and **B**. An appropriate number $N_{\mathbf{A}}$ of the **X**-sites are selected at random and assigned to be occupied by species **A** only, and the remaining $N_{\mathbf{B}} = N - N_{\mathbf{A}}$ **X**-sites are assigned to species **B**. We repeat this procedure many times to produce a large number of different random configurations. A GULP input file is written for each configuration, with a name that includes the configuration number. A script file to run all the GULP calculations in sequence is also written. In our work, the GULP and script files are transferred to a unix workstation, and the script file is executed in order to run the GULP energy minimization calculations for each configuration. This could also be performed on a PC under the Microsoft Windows operating system. After all configurations have been relaxed with GULP, the output files are transferred back into the spreadsheet environment. The relaxed values of the energy (together with other information such as the quality of the energy minimization constants) are then read back into a spreadsheet. Only configurations that have been successfully relaxed should be used in the subsequent analysis; with large configurations it is often found that some configurations do not relax without user intervention.

In parallel with the generation and execution of the many GULP files for the different atomic configurations, we have to determine all the variables that are required for the model Hamiltonian as outlined earlier in this paper. This means identifying all the different types of interactions that may be included within the Hamiltonian. These generally include: (1) the number of first, second, and more distant **A**—**A** neighbours; (2) in the case of differing crystallographic **X**-sites we have to count the number of **A** and **B** species on each type of **X**-sites; (3) in some cases, additional energy-terms, such as multi-site interactions.

The interactions are usually based on the distances between the atomic sites of the average crystal structure. For example, for the pair interactions, these are automatically ordered by the distances between sites. However, there are cases when symmetry (or just bad luck!) allows two distinct types of interaction to have the same distance, and so some attention may be needed to

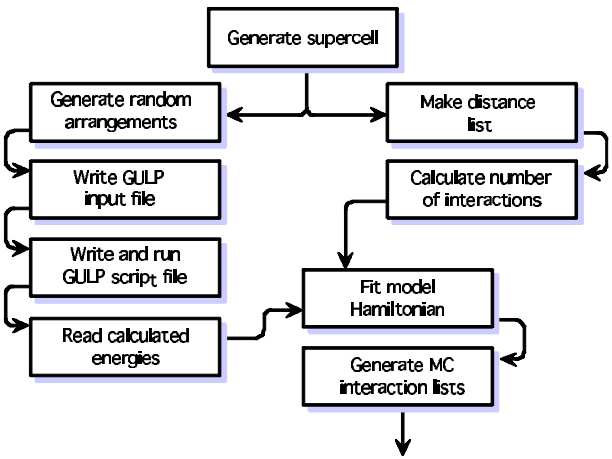

FIG. 6. Flow diagram illustrating the procedure of generating a file containing input data for a Monte Carlo simulation, from a crystal structure.

manually over-ride the automatic ordering of interactions based on distances and to separate distinct interactions with the same distance. For every configuration, the spreadsheet then counts the number of interactions. The information about which site is occupied by which species in each configuration is always stored in the spreadsheet. As a result, if it becomes necessary to extend the model, it is possible to return to this stage to determine additional variables from the stored information. It is also necessary to take account of the periodic boundary conditions. In some cases it may be unavoidable to have one atom interacting with another atom and its image in another unit cell, which will give a factor of two on the contribution from the bond energy.

To identify the important interactions and to determine the values of the J parameters, two built-in procedures of Excel, the Solver and the Multilinear Regression, can be used. The latter gives extensive information about the quality of the fitted model and the statistical relevance of the various J values, but is limited in the total number of adjustable parameters. Correlation between different J values can be quite high. Some experimentation in the choice of interactions to include may be required in order to identify insignificant interactions. The output from the Multilinear Regression analysis includes a number of significance parameters, which help guide this experimentation. High correlations between parameter values will give rise to large values of the standard errors on the fitted values of the exchange parameters. In such a case it will not be appropriate to merely remove all the correlated parameters simply because the regression indicates a high standard error. Correlation between parameter values is not a problem in the way that it is for some other data-fitting procedures: provided that a consistent set of interactions is used in subsequent applications, correlation has little effect. The only problems come when only a subset of a set of fitted interactions is used.

In complicated cases, where there are many exchange interactions, it can be useful to perform the fitting process in stages. For example, since the closest neighbours tend to have the strongest exchange interactions, it may be appropriate to obtain values for these first, and then extend the fitting procedure to include more distant interactions. To extend the example, if one had a layered structure, with strong exchange interactions within a layer but weak exchange interactions between layers, it may be appropriate to obtain values of the exchange interactions within the layers first, and then refine the model by including the exchange interactions between layers. If at any stage it appears that some of the exchange interactions do not have a numerical significance, these can be excluded in subsequent fits, and the procedures can be repeated until a satisfactory model has been obtained. On the other hand, it may turn out that the initial set of exchange interactions is not complete, and the model will then need to be extended in a subsequent fit.

At each stage the quality of the fit can be monitored by plotting the energy of the configurations calculated from the set of fitted values of E_0, J's and μ's against the corresponding lattice energy. We will show examples of these plots in the case studies given later. For a good fit, the points will be tightly clustered around the line passing though the origin with gradient of unity. The quality of the fit can be assessed using coefficients such as R^2, defined as

$$R^2 = 1 - \frac{\langle (\Delta E)^2 \rangle}{\langle E^2 \rangle - \langle E \rangle^2}$$

where E is the energy of a configuration, ΔE is the difference between the model energy and lattice energy of a configuration, and the angle brackets denote averages over all configurations. The numerator gives the variance of the differences between the fitted energies and lattice energies, which is normalized by the variance of the spread of energies of all configurations given in the denominator. Clearly, a value of R^2 close to 1 indicates the best fit.

There is one other hazard that the user needs to be aware of. It is possible for any structure to have different ordered states with similar energies, and the fitted model may give a lowest-energy ordered structure that is not the lowest-energy structure in the initial lattice energy minimization calculations. This is possible if there is a large sensitivity to small changes in the model parameters (as was found in work on Al/Si ordering in cordierite by Thayaparam *et al.*, 1996). One solution may be to include particular types of configurations in the model fitting procedure (with appropriate weightings) that highlight the differences in energy between different possible ordered structures. The point is that the model fitting cannot be treated as completely routine, and checks such as the ability of the final model to give the correct ordered structure as the lowest-energy structure are essential.

The final stage is to generate input files for subsequent Monte Carlo calculations. The important information that needs to be transferred to these files is the values of the interaction parameters and the neighbour lists that define the interactions. In complex materials, these neighbour lists can be quite extensive.

For the different tasks summarized above, several different Excel macros (modules) have been developed using VISUAL BASIC. These are available for downloading from the web site http://www.esc.cam.ac.uk/ossia. A manual for the use of these modules is also available from this web site. One note of caution is that the use of these modules is rarely completely automatic, and we have found that some small modifications are frequently needed when being used for a new system in order to take account of special cases that may arise! The procedures have been arranged that the output from one can be used for analysis in a different programming environment. For example, it may be useful to use a different fitting program to obtain the values of the exchange interactions and chemical potentials, particularly since the fitting procedure can be quite challenging in complex cases. However, one of the most useful features of the spreadsheet method is that all the tasks are managed within a common environment, and the spreadsheet is able to perform an important data-management task.

Case of three ordering atoms

When there are three ordering atoms rather than two, as outline as Case 4 in the previous section, there will be three times as many exchange constants to determine as in the case where there are only two ordering atoms. This may make for a complicated fitting procedure, particularly if there are many different types of interaction neighbours to take into account. We label the three types of atoms as **A**, **B** and **C** as before. From before, we require the three exchange interactions

$$J_{\mathbf{AA}} = (E_{\mathbf{AA}} + E_{\mathbf{BC}} - E_{\mathbf{AB}} - E_{\mathbf{AC}})$$
$$J_{\mathbf{BB}} = (E_{\mathbf{BB}} + E_{\mathbf{AC}} - E_{\mathbf{AB}} - E_{\mathbf{BC}})$$
$$J_{\mathbf{CC}} = (E_{\mathbf{CC}} + E_{\mathbf{AB}} - E_{\mathbf{AC}} - E_{\mathbf{BC}})$$

Some help may be gained by performing analysis with configurations containing only two types of atoms, which can give the two-atom exchange interactions (now specifically labelled by the superscript denoting the pairs of cations for clarity):

$$J^{(\mathbf{AB})} = E_{\mathbf{AA}} + E_{\mathbf{BB}} - 2E_{\mathbf{AB}}$$
$$J^{(\mathbf{AC})} = E_{\mathbf{AA}} + E_{\mathbf{CC}} - 2E_{\mathbf{AC}}$$
$$J^{(\mathbf{BC})} = E_{\mathbf{BB}} + E_{\mathbf{CC}} - 2E_{\mathbf{BC}}$$

We noted earlier that it follows from the constraints linking the numbers of pairs of atoms that it is not possible to extract separate values of the bond energies (such as $E_{\mathbf{AA}}$ and $E_{\mathbf{AB}}$). However, the two-atom exchange interactions will provide useful constraints. By forming appropriate combinations of the two-atom exchange constants, we have

$$J^{(\mathbf{AB})} + J^{(\mathbf{AC})} - J^{(\mathbf{BC})} = 2E_{\mathbf{AA}} + 2E_{\mathbf{BC}} - 2E_{\mathbf{AB}} - 2E_{\mathbf{AC}} = 2J_{\mathbf{AA}}$$

$$J^{(\mathbf{AB})} + J^{(\mathbf{BC})} - J^{(\mathbf{AC})} = 2E_{\mathbf{BB}} + 2E_{\mathbf{AC}} - 2E_{\mathbf{AB}} - 2E_{\mathbf{BC}} = 2J_{\mathbf{BB}}$$

$$J^{(\mathbf{AC})} + J^{(\mathbf{BC})} - J^{(\mathbf{AB})} = 2E_{\mathbf{CC}} + 2E_{\mathbf{AB}} - 2E_{\mathbf{AC}} - 2E_{\mathbf{BC}} = 2J_{\mathbf{CC}}$$

If an appropriate set of two-atom configurations is combined with the set of three-atom configurations, the database of configuration energies may be sufficiently constrained to enable the fitting procedure to be stable even with many different types of interaction. Of course, this relies on there being no non-analytic dependence of the exchange interactions on chemical composition.

Case studies

Al/Si ordering energies in framework aluminosilicates

From a number of studies, we now have a large database of values for the first and distant neighbour Al/Si tetrahedral exchange interactions of a wide range of aluminosilicates (Bertram *et al.*, 1990; Dove *et al.*, 1993; Thayaparam *et al.*, 1994, 1996; Myers 1999; Palin *et al.*, 2001). The nearest-neighbour values are shown graphically in Fig. 7. The range of examples includes cases where the nearest-neighbour interactions lie within chains, sheets or within a three-dimensional framework.

The important point that emerges from Fig. 7 is that the range of values of the nearest-neighbour exchange interactions is quite large. If the main component of the interaction was purely electrostatic in origin due to the charge difference between Al^{3+} and Si^{4+} cations, such a range may not have been expected. However, the range of values points to the importance of the effects of

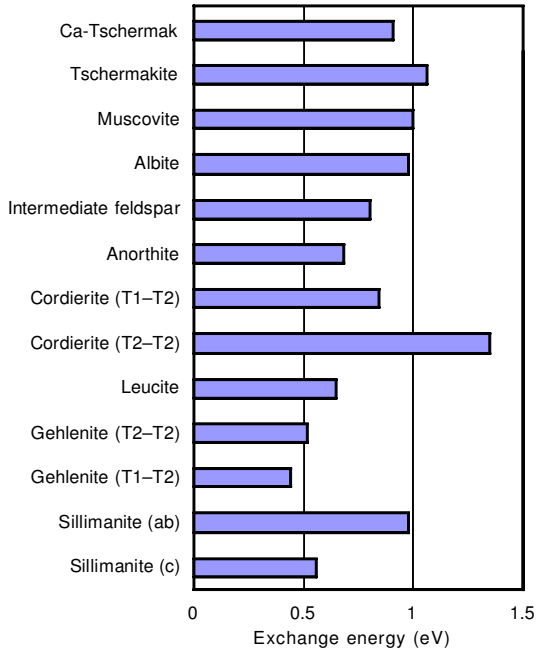

FIG. 7. Graphical representation of the nearest-neighbour Al/Si exchange interactions for a range of aluminosilicate crystals, calculated using empirical model interatomic interactions. In some cases there are two distinct nearest-neighbour interactions, either because there are two distinct tetrahedral sites or simply because of the structure topology – these are discussed in the corresponding references. References for the data are, sillimanite, Al_2SiO_5: Bertram *et al.* (1990); leucite, $KAlSi_2O_6$: Dove *et al.* (1993); gehlenite, $Ca_2Al_2SiO_7$: Thayaparam *et al.* (1994); cordierite, $Mg_2Al_4Si_5O_{18}$: Thayaparam *et al.* (1996); the feldspars anorthite, $CaAl_2Si_2O_8$, albite, $NaAlSi_3O_8$, and one of intermediate composition $Ca_{0.5}Na_{0.5}Al_{1.5}Si_{2.5}O_8$: Myers (1999); muscovite, $K_2Al_4(Si_6Al_2O_{20})(OH)_2$: Palin *et al.* (2001); Ca-Tschermak pyroxene, $CaAl_2SiO_6$ and tschermakite amphibole, $Ca_2(Mg_3Al_2)(Si_6Al_2)O_{22}(OH)_2$: our unpublished data.

local stress fields arising from the mismatch in size between the Al^{3+} and Si^{4+} cations. For first-neighbour interactions, these effects are reduced if the arrangement maximizes the number of neighbours being cations of different size. The relative sizes of the effects of the localized stress fields and the electrostatic contributions have been identified by McConnell *et al.* (1997) using Al/Si ordering in kalsilite as a specific test case. Different structures have different abilities to accommodate local stress fields, with different ways of forming localized strain distortions. This accounts for the range of values of the exchange interactions.

The same discussion is also relevant for second and more distant neighbour exchange interactions. We compare the exchange interactions for six-membered rings of tetrahedra in the framework structure cordierite, $Mg_2Al_4Si_5O_{18}$ (Thayaparam *et al.*, 1996), in the sheet silicate muscovite, $K_2Al_4(Si_6Al_2O_{20})(OH)_2$ (Palin *et al.*, 2001), and in the amphibole tschermakite, $Ca_2(Mg_3Al_2)(Si_6Al_2)O_{22}(OH)_2$, which contains ribbons of six-membered rings of tetrahedra (our own unpublished data). In Fig. 8, we show the definitions of the three exchange interactions, and chart the values for the different examples. Clearly there is a significant variation between the different structures.

Recent work on Al/Si ordering in muscovite (Palin *et al.*, 2001) illustrates many aspects of the approach to modelling Al/Si ordering. Muscovite is a layer silicate. The structure has sandwiches of two layers of tetrahedral sites of composition $AlSi_3$, separated by a layer of octahedral sites containing Al cations. Two sandwiches are separated by a layer of K cations, which gives charge balance. The structure is shown in Fig. 9. Fifty configurations were used to calculate the

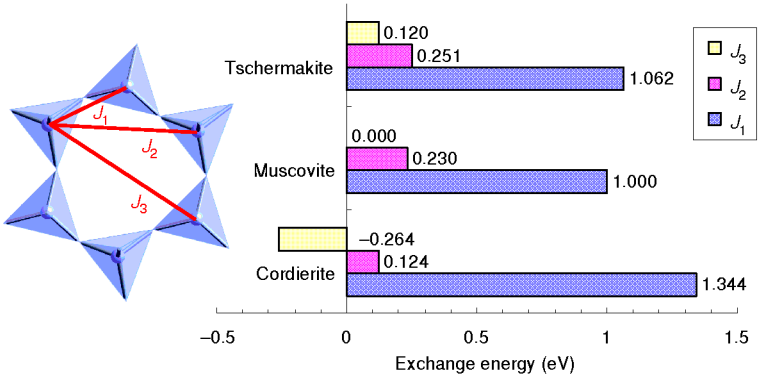

FIG. 8. (Left) The definition of the first-, second- and third-neighbour interactions, J_1, J_2 and J_3, within a 6-membered ring of tetrahedra. (Right) Graphical representation of the values of J_1, J_2 and J_3 within 6-membered rings of tetrahedra for a number of different aluminosilicate crystals, calculated using empirical model interatomic interactions. References for the data are, cordierite, $Mg_2Al_4Si_5O_{18}$: Thayaparam *et al.* (1996); muscovite, $K_2Al_4(Si_6Al_2O_{20})(OH)_2$: Palin *et al.* (2001); tschermakite, $Ca_2(Mg_3Al_2)(Si_6Al_2)O_{22}(OH)_2$: our unpublished data.

ordering energies. The first stage was to determine the exchange interactions within a single layer of tetrahedral sites. It was necessary to define exchange interactions to the fourth neighbour in any layer in order to be able to uniquely define an ordered Al/Si arrangement within a layer. The layer interactions are shown in Fig. 9. The fitting procedure gave positive values for J_1, J_2 and J_4, and a near-zero value for J_3 (the values for J_1–J_3 are given in Fig. 8, and for comparison the value of J_4 was 0.13 eV). The values of the exchange interactions led to the proposal for the ordered structure shown in Fig. 9. In fact without the inclusion of J_4 there are several possible ordered structures, and the sign and value of J_4 is crucial for differentiating between them. Exchange interactions were also defined between tetrahedral sites in different layers to give the full three-dimensional nature of ordering processes. Most of these were quite weak, with values below that of J_1 (1.0 eV) and J_2 (0.23 eV), although one interlayer exchange interaction had a value higher than that of J_2 (0.38 eV). The quality of the fit is shown graphically in Fig. 10.

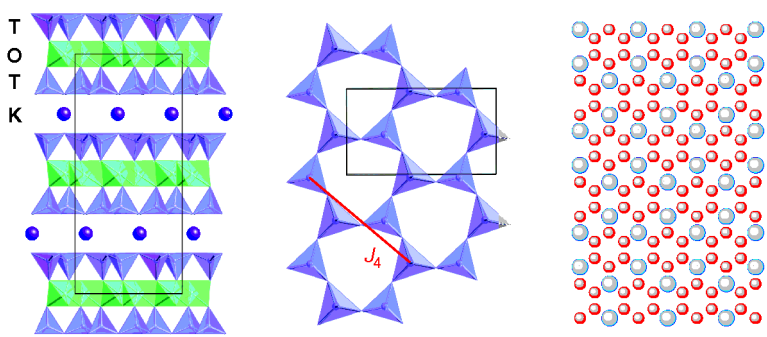

FIG. 9. (Left) Crystal structure of muscovite, $K_2Al_4(Si_6Al_2O_{20})(OH)_2$, showing the layers of tetrahedral sites either side of a layer of octahedral sites, and K cations in the interlayer space. (Centre) A single layer of tetrahedral sites in muscovite showing the J_4 exchange interactions (the exchange interactions J_1, J_2 and J_3 are defined in Fig. 8). (Right) The proposed Al/Si ordering on the tetrahedral sites based on the values of the exchange interactions, where the Al cations are shown as the larger spheres and Si as the smaller spheres (after Palin *et al.*, 2001). The Al cations are in a hexagonal arrangement that has Al cations with J_3 interactions but avoiding J_1, J_2 and J_4 interactions.

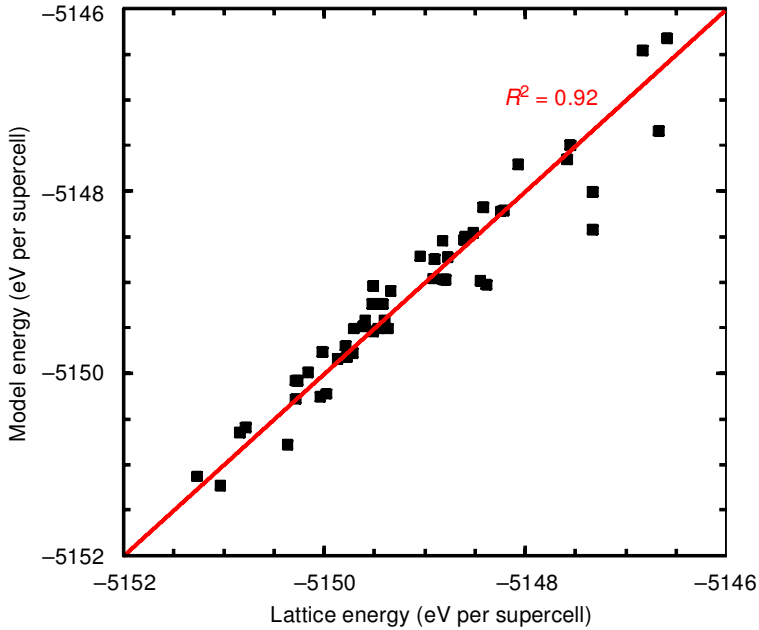

FIG. 10. Graphical representation of the quality of the fitted exchange interactions in the model for muscovite, shown as a plot of lattice energy calculated using GULP *vs.* energy of parameterized model. The points represent each of the configurations used in the analysis. The straight line has unit gradient and passes through the origin, and ideally the points should be closely scattered about this line (Palin *et al.*, 2001).

Pyrope—grossular solid solution

One of the most important mineralogical solid solutions is that between the garnets pyrope, $Mg_3Al_2Si_3O_{12}$, and grossular, $Ca_3Al_2Si_3O_{12}$. A number of interactions involving the exchange of the Mg^{2+} and Ca^{2+} cations between dodecahedral sites can be identified, and are shown in Fig. 11. The exchange interactions are labelled according to the intersite distance. The purpose in determining the exchange interactions was to be able to study the thermodynamic properties and short-range structure of the solid solution. The calculation of the exchange interactions was carried out for several compositions, including the dilute limits where in a supercell containing N Mg/Ca cations there were only two cations of one species and $N - 2$ cations of the other species (Bosenick *et al.*, 2000). The results showed that the exchange interactions did not vary significantly with composition, and there was no obvious asymmetry between the Mg-rich and Ca-rich ends of the solid solution. The fitted exchange energies for different compositions, and the quality of fit for the 50:50 mixture, are plotted in Fig. 12.

The interesting point that emerged from the calculations is that the strongest interaction was, in fact, the third-neighbour interaction, with only the fourth- and fifth-neighbour interactions having appreciable exchange energies. The first- and second-neighbour interactions were close to zero. At first sight, this is surprising, since we are used to thinking that nearest-neighbour interactions are always the strongest. However, in the case of the garnet structure the third-neighbour interaction involves directly applying a force to an SiO_4 tetrahedron that lies exactly between two third-neighbour sites; this is indicated in Fig. 11. This force acts to distort the tetrahedron rather than to simply cause it to rotate, and therefore it corresponds to the large exchange energy. The third-neighbour linkages lie in one-dimensional chains rather than having a three-dimensional connectivity, and for this reason there is no Mg/Ca site-ordering phase transition in the solid solution, at least not at sufficiently high

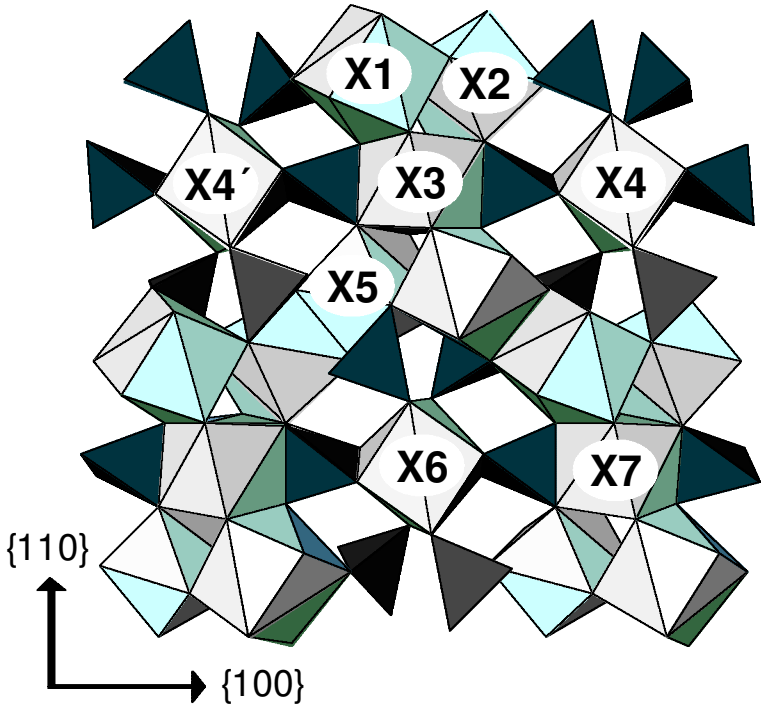

FIG. 11. Crystal structure of garnet, showing the dodecahedral framework and its linkage to the SiO_4 tetrahedra. The AlO_6 octahedra are not shown for clarity. The exchange interactions between the dodecahedral sites (marked as **X1** to **X7**) correspond to the following different distances (which are defined for use in Fig. 12): d_1 between **X1 − X2**; d_2 between **X2 − X4**; d_3 between **X3 − X4**; d_4 between **X1 − X5**; d_5 between **X2 − X5**; d_6 between **X3 − X6**; d_7 between **X3 − X7** (after Bosenick *et al.*, 2000).

temperatures to allow the thermodynamic driving force to overcome the kinetic barriers. The basic result obtained using the empirical interatomic potentials was confirmed using a set of selected quantum mechanical calculations performed using the SIESTA code (as described in Bosenick *et al.*, 2001).

Pyroxene solid solutions

The diopside–Ca-Tschermak solid solution, $Ca[Mg_xAl_{1-x}]^{VI}[Si_{1+x}Al_{1-x}]^{IV}O_6$ is a good challenge for the approach we have developed in this paper. In the Ca-Tschermak end-member, $x = 0$, there is Si/Al ordering on the tetrahedral sites (labelled with the superscript IV in the chemical formula) with equal numbers of the two types of cations. For other members of the solid solution ($x < 1$), there is also Mg/Al ordering on the octahedral (VI) sites in addition to the Si/Al ordering on the tetrahedral sites. We therefore need to determine exchange interactions for the ordering on the tetrahedral and octahedral sites, and for interactions between these types of sites. The crystal structure is shown in Fig. 13, which also shows the exchange interactions used in this work,

The development of the model followed the following stages. First, the exchange interactions involving the tetrahedral ordering in the pure Ca-Tschermak end-member were constructed. The dominant interaction found is the Al–Al repulsion between corner sharing $(Al,Si)O_4$ tetrahedra in the tetrahedral chains. In addition, weaker exchange interactions exist between neighbouring tetrahedral chains. These are responsible for the ordering between neighbouring chains and hence for the long-range ordering behaviour of Ca-Tschermak. In the case of complete Al-avoidance, there are four possible different fully ordered Ca-Tschermak structures with space group $C2$, $C\bar{1}$, $P2/n$ and $P2_1/n$ (Okumara *et al.*, 1974). To date, none has been

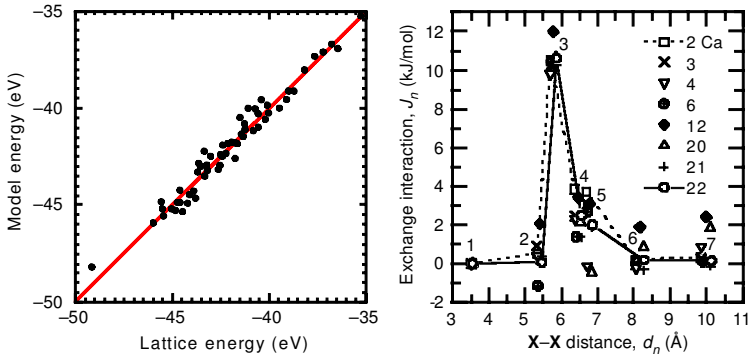

FIG. 12. (Left) Graphical comparison of the quality of the fitted model interactions for Mg/Ca site exchange in the 50:50 pyrope–grossular solid solution. (Right) Graphical representation of the values of the exchange interactions for supercells containing different numbers of Ca cations in a supercell of 24 dodecahedral sites (the numbers in the legend give the number of Ca cations). The number n of the exchange interactions is given with each group of points (after Bosenick *et al.*, 2000).

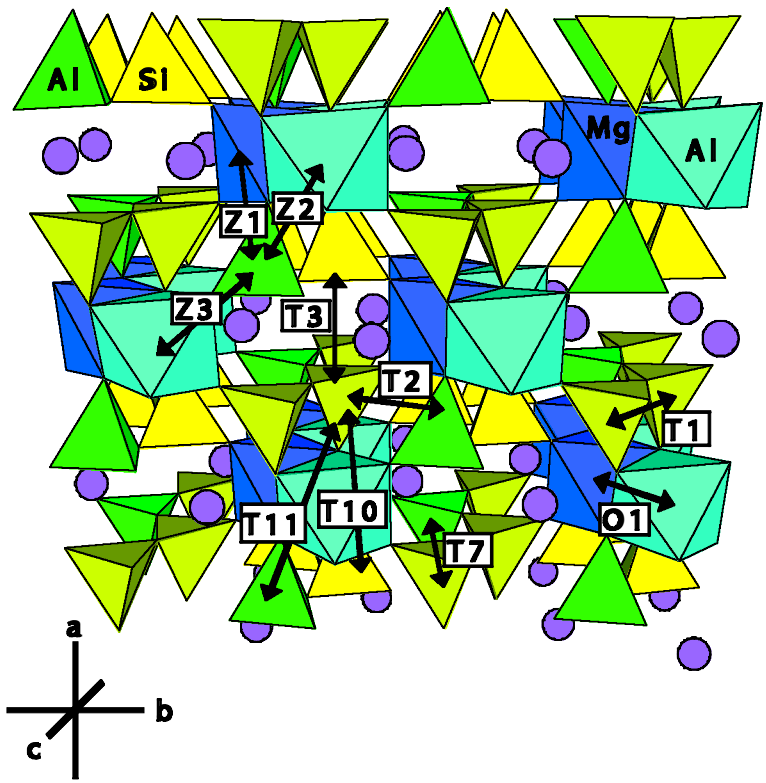

FIG. 13. Crystal structure of pyroxene, showing the important exchange interactions within the diopside–Ca-Tschermak solid solution, $Ca[Mg_xAl_{1-x}]^{VI}[Si_{1+x}Al_{1-x}]^{IV}O_6$. The exchange interactions labelled T1 to T11 represent interactions between tetrahedral sites, O1 represents the interaction between nearest-neighbour octahedral sites, and Z1 to Z3 represent interactions between a tetrahedal and an octahedral site.

observed experimentally but according to our simulations, the energetically most favourable structure is that of symmetry $P2_1/n$. Monte Carlo simulations (Bosenick *et al.*, 1999; Warren *et al.*, 2001) suggest that the phase transition is expected at around 1000 K. However, at these low temperatures Ca-Tschermak is thermodynamically unstable with respect to transformation to grossular and Al_2O_3 (Gasparik, 1984).

In a second step, the exchange interactions between the octahedral sites were identified. Simulations were run on diopside-rich solid-solutions in which the Si/Al distribution on the tetrahedral sites was modelled as an average site distribution using the virtual crystal approximation (discussed above), while the Mg/Al cations distributed on the octahedral sites were treated as discrete cations. This trick allowed a separation and hence an identification of octahedral exchange interactions without any coupling to tetrahedral–tetrahedral and tetrahedral–octahedral interactions. The main exchange interaction is again a repulsion between neighbouring sites, albeit a factor of 2–3 times smaller than in the case of the tetrahedral interactions. Additional interactions between neighbouring octahedral chains were found to be very weak and were therefore neglected.

The last set of simulations were performed on diopside–Ca-Tschermak solid solutions of different compositions. Here, all cations, i.e. Al and Si on tetrahedral sites and Mg and Al on octahedral sites, were treated as discrete cations. Since the tetrahedral and octahedral interactions had been determined in the first two steps, the third step allowed the determination of the tetrahedral–octahedral exchange interactions. In contrast to the interactions amongst the tetrahedral sites and octahedral sites themselves, which were positive and hence of repulsive nature, the interaction between tetrahedra and octahedra is negative and hence of attractive nature. This means that it favours Al in both of the neighbouring tetrahedral and octahedral sites.

In the beginning, a separate analysis of each dataset for the different compositions enabled the identification of the dominant exchange interactions plus the determination of their approximate values. In the final stage all data of all compositions were collected and a consistent set of interaction exchange parameters was determined. The final plot of the fitted energies is shown in Fig. 14, where we also give the energies of the different exchange interactions. The plot shows that the fitting of the exchange energies over a range of compositions has produced a consistent set of exchange interactions, and we have no clear dependence of the interactions on the composition variable. These have been used in Monte Carlo simulations to determine the resultant ordered structures and to interpret NMR data, as described in the following paper (Warren *et al.*, 2001).

Micas and other 2:1 layer silicates

The simulations of layer silicates follow the same challenges as in pyroxene. Here we consider the general case represented by the formula $M_{x+y}(Al_{4-x}Mg_x)(Si_{8-y}Al_y)(OH)_4O_{20}$, M = Na,K. The case $x = 0$, $y = 2$ is that of muscovite, for which the work on Al/Si ordering was discussed earlier (Palin *et al.*, 2001). The challenge is to determine the exchange interactions associated with Al/Mg ordering within the octahedral layers, and the coupling interactions between the octahedral and tetrahedral layers.

The approach taken was to build upon the work on Al/Si ordering in muscovite. In a separate task we computed Mg/Al cation exchange interactions within the octahedral layers of smectite/illite. We used a system with x = 1 in the chemical formula given above, to give the composition $MgAl_3$ in the octahedral layer. We set $y = 0.28$ and $y = 0.8$ in separate simulations, and used Na as the interlayer M cation in both cases, and also K for the $y = 0.8$ simulation. The arrangement of octahedral sites is exactly the same as the arrangement of tetrahedral sites shown in Fig. 9. The same four exchange interactions shown in Figs 8 and 9, but now for Al/Mg ordering, were considered. The Al/Si cation arrangements in the tetrahedral sheets were assumed to be random and approximated by the virtual crystal method, as was done in the intermediate stage of developing models for the pyroxenes (discussed above). For each composition, nearby 90 configurations with different ordering level of the octahedral cations were calculated using a $2 \times 2 \times 1$ supercell. The results for J_1 to J_3 are given in Fig. 8; for comparison, the value of J_4 was 0.13 eV, similar in size to the other exchange interactions.

The fitted values of the exchange interactions for $Na_{1.28}(Al_3Mg_1)(Si_{7.72}Al_{0.28})(OH)_4O_{20}$ were 0.65(1), 0.16(1), 0.09(1), 0.015(9) eV for J_1, J_2, J_3, and J_4 respectively (errors associated with parameter correlation given in brackets), which are only slightly lower overall than the corresponding

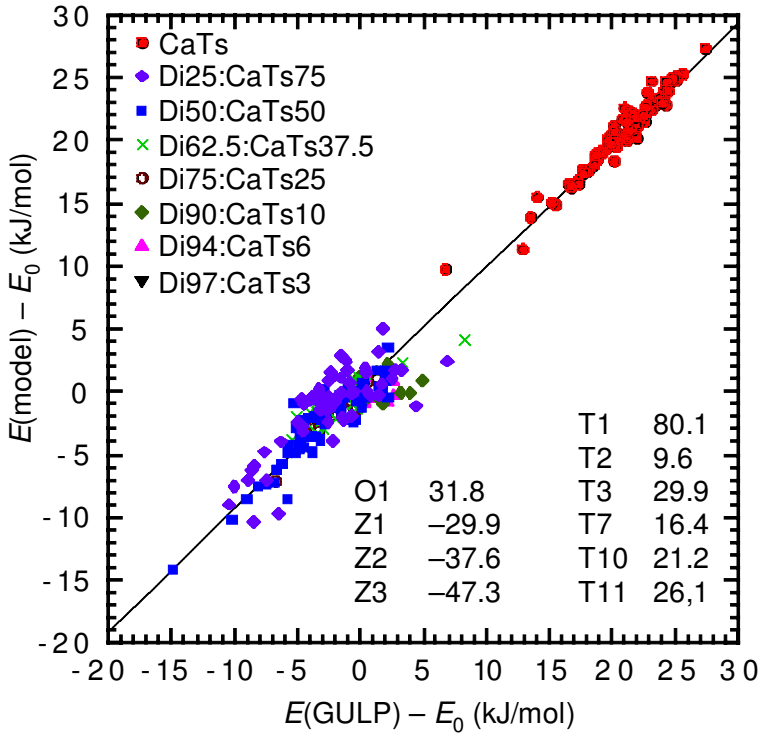

FIG. 14. Comparison of the GULP energies and the fitted model Hamiltonian of the diopside–Ca-Tschermak solid solution. The model takes account of Al/Si site exchange interactions across the tetrahedral sites, Al/Mg site exchange interactions across the octahedral sites, and Al–Al interactions between the octahedral and tetrahedral site, as defined in Fig. 13. The points (defined in the upper right corner) represent configurations of different compositions, and the values of the fitted exchange interactions are given on the lower right side.

values for Al/Si ordering in the tetrahedral layer. Replacing Na by K as the interlayer cation, and increasing the tetrahedral charge, did not produce significant changes in the exchange interaction values: the values of the four exchange interactions averaged over all three simulations are 0.64(2), 0.16(1), 0.08(1) and 0.023(8) eV respectively, with standard deviations from the average given in brackets. The variations of the fitted values of the exchange constants between samples are of the same order as the correlation errors on the individual parameter values. Note that the exchange interactions follow the same pattern as in the tetrahedral layers, and will predict the same ordering as in the tetrahedral layers. As an aside, the procedure was repeated for a composition Al_3Fe^{3+} in the octahedral layer, giving exchange interactions that are an order of magnitude lower (values 0.025(1), 0.007(1), 0.003(1) and 0.0025(11) eV respectively).

Finally, using the fitted values of the Al/Si^{IV} and Mg/Al^{VI} exchange interactions, we also determined values of the interactions between the tetrahedral and octahedral layers appropriate for the study of coupled ordering processes in phengite, $K_2(Al_3Mg)(Si_7Al)O_{22}(OH)_4$ ($x = 1$, $y = 1$ in the general formula given above). This is now a case of having three ordering cations, but with the restriction that there are two types of cation in one network (tetrahedral sites) and two types in the second network (octahedral sites). This corresponds to Case 3 in the section 'Basic Theory'. We defined four tetrahedral–octahedral interactions based on distance, and computed the exchange interaction based on the number of Al–Al pairs on any two sites. The exchange interactions are defined in Fig. 15. It was found that the interaction labelled J_c was weak (value 0.03 eV), whereas the values of the other exchange interactions were strong and negative

(of order −1 eV). This implies that the interactions between tetrahedral and octahedral sites favours having Al neighbours. The importance of this will be shown in the Monte Carlo simulations in the following paper (Warren *et al.*, 2001), where it was found that these coupled interactions overcome the natural ordering process in the octahedral layer to produce a more complex ordered structure.

Mg/Al ordering (octahedral) and Al/Si ordering (tetrahedral) in amphiboles

An ongoing project on cation ordering in amphiboles highlights a number of the points made earlier in this paper. In amphiboles there is both Al/Si ordering in chains of tetrahedral sites, and Mg/Al ordering in chains on octahedral sites. In this regard the situation is similar to the coupled ordering in the micas and pyroxenes discussed above, although the two points that we illustrated are not with regard to the coupled processes.

The exchange interactions were obtained for Mg/Al ordering in the octahedral sites in glaucophane, $Na_2(Mg_3Al_2)Si_8O_{22}(OH)_2$. There are three distinct octahedral sites, as shown in Fig. 16. This is an example of the need for the inclusion of chemical potential terms, as outlined in Case 2 in the 'Basic Theory' section. The fit of the model Hamiltonian was quite reasonable. One result was that the energy of placing an Al cation on the **M1** site was the same as that for the **M3** site, so a single chemical potential associated with an Al cation moving onto an **M2** site was used in the final model. A positive value (0.36 ± 0.08 eV — the error represents correlations with the values of other parameters in the model) was obtained, which by itself makes it unfavourable for Al cations to be on the **M2** sites. This is contrary to experimental data (Hawthorne, 1997), which suggest that the **M2** site is in fact the site preferred by the Al cations. Of course, the chemical potential term is not the only term. The relevant exchange interactions are defined in Fig. 16, and by themselves these exchange interactions would prefer to have the Al cations on the **M2** sites. The point is illustrated in Fig. 17, where we compare the energies of four configurations graphically. Two of these are ordered structures with all the Al cations on the **M1** sites and all the Al cations on the **M2** sites. The other two

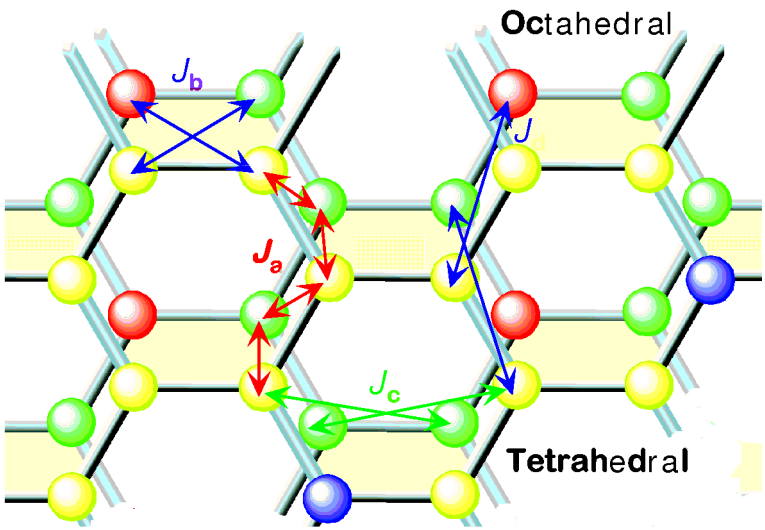

FIG. 15. Representation of a pair of neighbouring tetrahedral (upper layer, yellow and blue spheres) and octahedral layers (lower layer, red and green spheres) of cation sites in phengite, $K_2(Al_3Mg)(Si_7Al)O_{22}(OH)_4$, showing the four different exchange interactions computed in the analysis described in the text. In the tetrahedal layer, the yellow spheres represent Si cations and the blue spheres represent Al cations. In the octahedral layer, the green spheres represent Al cations and the red spheres represent Mg cations. The arrangement of cations in the two layers is the ordered structure obtained using Monte Carlo simulations (Warren *et al.*, 2001).

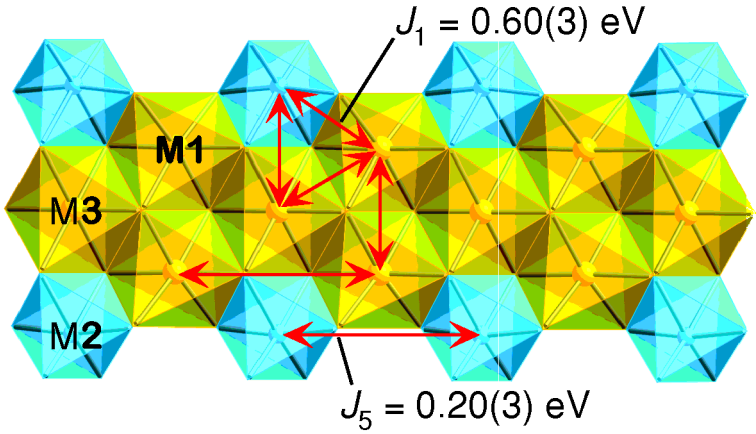

FIG. 16. Ribbons of octahedral sites in glaucophane, $Na_2(Mg_3Al_2)Si_8O_{22}(OH)_2$, labelled M1, M2 and M3. The yellow and blue octahedra represent sites occupied by Mg and Al cations respectively in the ordered structure. The figure shows some of the significant fitted values of the exchange interactions for Mg/Al ordering, with errors in brackets.

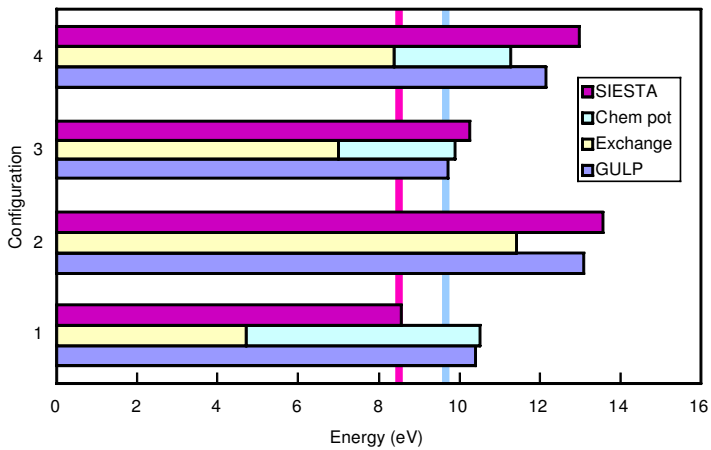

FIG. 17. Comparison of energies of four configurations of Mg and Al cations in glaucophane, $Na_2(Mg_3Al_2)Si_8O_{22}(OH)_2$. Configurations #1 and #2 have Al cations in only M2 and M1 sites respectively, whereas configurations #3 and #4 both have half of the Al cations in M1 and M2 sites. The lowest bar for each configuration represents the lattice energy calculated using the GULP code, with the constant E_0 obtained in the fitted model subtracted. The middle bar represents the energy of the fitted model (minus E_0), which is divided into contributions from the chemical potential and the exchange interactions (note that there is no contribution from the chemical potential in configuration #2). The top bar represents the energy calculated by quantum mechanics methods using the SIESTA code (with a constant value subtracted). The blue vertical line indicates the lowest energy of all four configurations from the GULP calculations (configuration #3), and the maroon vertical line indicates the lowest energy from the SIESTA calculations (configuration #1). The point of the comparison is that the SIESTA calculation gives the experimental ordered structure as the lowest-energy structure, whereas the GULP calculation finds another configuration with lower energy. On the other hand, the exchange interactions alone give the experimental ordered structure as the lowest-energy structure, and the value of the SIESTA calculations is that they can give corrections to the value of the chemical potential.

configurations have half the Al cations on **M1** sites and half on the **M2** sites. In Fig. 17 we show the raw lattice energies, the model energies, the chemical potential energies, and the sums of the exchange energies. It is clear that the exchange interactions are sufficiently strong to overcome the chemical potential energies and favour **M2** ordering of the Al cations over **M1** ordering. However, one of the configurations with Al cations distributed across both the **M1** and **M2** sites has a lower overall energy that the configuration with pure **M2** ordering, both in the raw lattice energy and the model Hamiltonian. This is possible because there is a fine balance between the energies of the chemical potential and exchange interactions.

The problem with the disagreement between the predicted ordering pattern (Al in both **M1** and **M2** sites) and the observed ordering pattern (Al only in **M2** sites, Hawthorne, 1997) is likely to arise because of problems with the empirical interactions. These are likely to give reasonable values for the exchange interactions if these are determined by strain effects associated with size mismatch, but, as we have already mentioned, it is possible for the empirical models to give inaccurate relative energies of cations in different sites when these differences are small. The solution was to use quantum mechanical calculations. However, with 328 atoms in the unit cell of the samples being studied, such calculations are on a scale that is far beyond the scope of routine calculations. The SIESTA code was used to calculate the energies of the four configurations, using minimal basis sets (more sophisticated basis sets would be too demanding). The energies given by these calculations are shown in Fig. 17. It can be seen that the calculations now give the structure with the Al cations ordered on the **M2** sites only as the lowest energy structure, in agreement with experiment (reference). Assuming that the values of the exchange interactions obtained from the empirical potentials are satisfactory, it is possible to subtract the exchange energies from the SIESTA results in order to obtain estimates for the chemical potential associated with the **M2** site. From the four configurations we estimate a value of -0.20 ± 0.13 eV; in this case the error arises from the fact that there is not complete consistency between the quantum mechanical and empirical calculations. However, all configurations give a negative value of the chemical potential for the Al cations on the **M2** sites, in contrast to the positive value given by the empirical models. SIESTA calculations with more configurations, or attempts to use more accurate basis sets, would tie down the value of the chemical potential more accurately. This example shows how it may be possible to combine calculations of exchange interactions from empirical model potentials with chemical potentials obtained from quantum mechanical calculations.

To obtain the interactions for the coupled system, the interactions for the tetrahedral network were obtained as a separate operation. Calculations were performed on tschermakite, $Ca_2(Mg_3Al_2)(Si_6Al_2)O_{22}(OH)_2$. The disorder in the octahedral sites was represented using the virtual crystal approximation. The chains of tetrahedral sites are shown in Fig. 18, together with the definitions (and fitted values) of some of the exchange interactions. There are two tetrahedral sites, and this necessitated the use of a chemical potential. In fact, the fitted value of the chemical potential (-0.56 eV) was large enough to favour the location of the Al cations on the **T1** sites, in accord with experiment (Oberti *et al.*, 1995). In this case the empirical models have obtained the correct sign for the chemical potential! The values of the exchange interactions shown in Fig. 16 are positive (numerical values given in Fig. 8), which suggests that the lowest-energy ordered structure has alternate Al cations in the **T1** sites on opposite sides of the ribbons of tetrahedral sites, as shown in Fig. 18. The exchange interactions in the *a* direction are all positive, and of similar size, which means that there is only a weak residual ordering interaction between ribbons in this direction. Moreover, the exchange interactions between ribbons in the third direction (*b*) are also weak. Overall, it appears unlikely that complete three-dimensional ordering in natural samples, beyond a preference of the Al cations for the **T1** sites, is unlikely. This example has highlighted the possibility to obtain simple insights from the values of the parameters in the model energy function directly before the need to resort to more detailed Monte Carlo calculations.

Spinel

Our final example is that of Mg/Al ordering across both the octahedral and tetrahedral sites in spinel, $MgAl_2O_4$. In this case, the disordering process does not involve a change in crystal symmetry, but involves a change in the

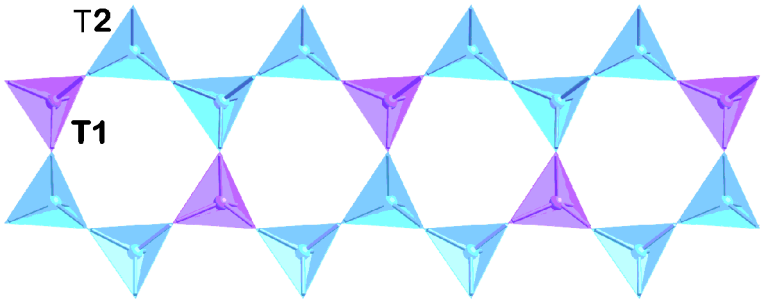

FIG. 18. The ribbons of tetrahedral sites in tschermakite, $Ca_2(Mg_3Al_2)(Si_6Al_2)O_{22}(OH)_2$. The pink sites represent the sites occupied by the Al cations in the ordered ribbons according to the fitted model, and the blue sites represent those occupied by the Si cations.

partitioning of the cations between the tetrahedral and octahedral sites. This is an example of a non-convergent ordering process (Carpenter *et al.*, 1994; Carpenter and Salje, 1994), and although it has many features of a phase transition, there is no specific ordering temperature. Because the main ordering process involves atoms changing their coordination, it is highly unlikely that empirical interatomic potential models could realistically describe the changes in energy associated with such a change. Therefore, the model for the ordering process in spinel required the use of *ab initio* quantum mechanics models. We used the CASTEP/CETEP codes (Payne *et al.*, 1992; Clarke *et al.*, 1992) to calculate the energies of a relatively small number of configurations of atoms.

Because of the small number of configurations, the number of parameters in the model Hamiltonian would necessarily be limited, and some experimentation was required to find the minimal set that would reproduce the calculated energies to a reasonable level. A good model was obtained by incorporating the exchange energy associated with cations moving between tetrahedral and octahedral sites and a single exchange interaction between nearest-neighbour tetrahedral and octahedral sites, and a three-site term. We identified two likely three-site terms, based on the three polyhedra (tetrahedra T, or octahedra O) linked at a common oxygen atom (Fig. 19).

Only the T–O–O term was found to be significant. The final model had only three adjustable parameters (plus a zero-energy term), but was capable of representing the quantum mechanical energies with reasonable accuracy, as seen in Fig. 20. Further details of the development of the model are given by Warren *et al.* (2000*a,b*).

The model Hamiltonian was used for Monte Carlo simulations (Warren *et al.*, 2000*a,b*, 2001). The results for the order parameter are shown in

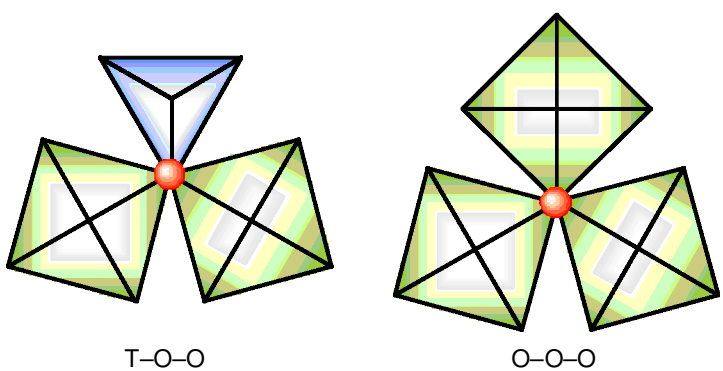

FIG. 19. Model of Mg/Al ordering across both the octahedral and tetrahedral sites in spinel.

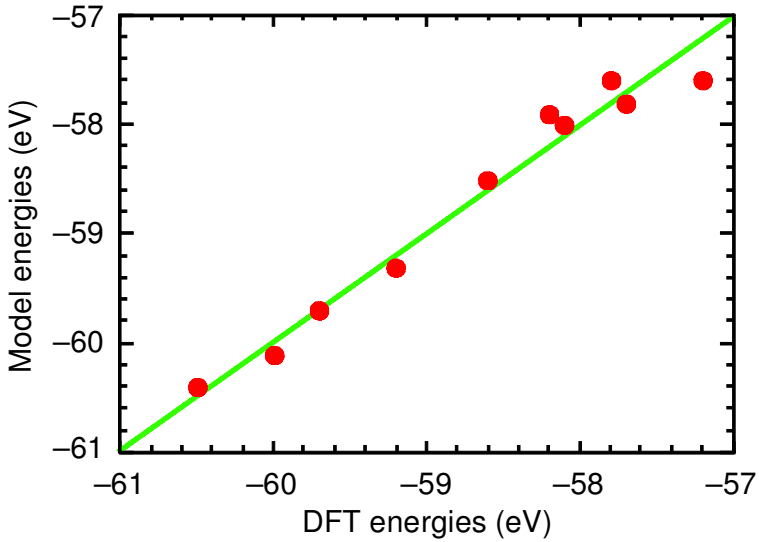

FIG. 20. Graphical representation of the quality of the agreement between the energies of the fitted Hamiltonian and the energies given by the quantum mechanics calculation for Mg/Al ordering in spinel, $MgAl_2O_4$ (Warren *et al.* 2000*a*,*b*).

Fig. 21, where they are compared with data obtained by neutron diffraction (Redfern *et al.*, 1999). The important point from the comparison is that the calculated temperature-dependence of the order parameter is in close agreement with the experimental data. The agreement is not perfect, but since the model calculations were developed without any account being taken of experimental data, the close agreement is a remarkable validation of the whole procedure.

Conclusions

In this paper, we have outlined an approach to determining the interactions involved in the exchange in the site positions of different types of cations in crystal structures. We have shown for several different types of systems how the energies can be expressed in terms of a few parameters within a model Hamiltonian. The results of the fitting of these parameters to large databases of energies of configurations have shown that the approach gives a reasonable representation of the ordering energies. We have also outlined issues associated with the use of empirical or quantum mechanical methods to describe the interactions between cations.

A number of important physical principles have emerged from this study. One is that it is not possible to transfer exchange interactions between different crystal structures. The main example highlighted in this paper is that the energies associated with Al/Si ordering are very different for different crystal structures. This indicates that the energies are determined by the particular ability of the crystal structure to distort to accommodate the local strains associated with the mismatch in size between the Al and Si cations, and are not as general one might have imagined. A second important principle is that the exchange energies can be relatively constant across a solid solution, although this may not always be the case. We have found that the cation ordering interactions in the pyrope–grossular, diopside–Ca-Tschermak, and mica series are independent of composition, but that there are systematic variations in the interactions for Al/Si ordering in the albite–anorthite series.

Acknowledgements

This research has been supported by NERC (GR3/10606), the EU (Marie Curie fellowship to AB), the Royal Society (travel support for CISD), and Acciones Integradas (UK/Spain joint programme giving travel support for CISD and MTD). We are grateful to Julian Gale (Imperial College, London) for assistance, and for providing his GULP code.

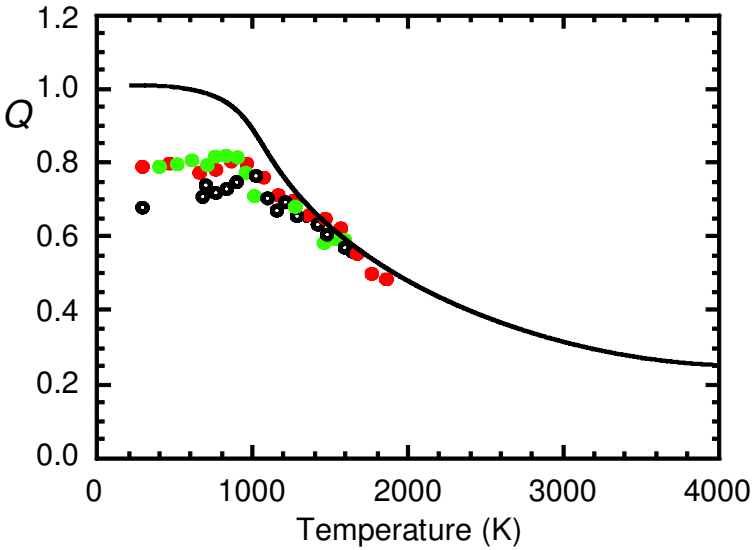

FIG. 21. Comparison of the order parameter associated with the non-convergent ordering of Mg and Al cations in spinel calculated by Monte Carlo simulations using the model Hamiltonian described in the text (continuous curve, Warren *et al.*, 2000*a,b*, 2001) and the experimental data of Redfern *et al.* (1999). The experimental data are affected by kinetics at temperatures below 700 K, and should not be taken into the comparison at these temperatures. Different experimental runs (corresponding to different thermal history of each sample) are indicated by different colours – the different behaviour at low temperatures shows the effects of ordering kinetics.

The quantum mechanics calculations were performed on the parallel computers of the Cambridge High Performance Computing Facility (funded by EPSRC and the University of Cambridge). A thoughtful review by Richard Harrison is greatly appreciated.

References

Artacho, E., Sánchez-Portal, D., Ordejón, P., García, A. and Soler, J.M. (1999) Linear-scaling ab-initio calculations for large and complex systems. *Physica Status Solidi (b)*, **215**, 809–17.

Allan, N.L., Barrera, G.D., Fracchia, R.M., Pongsai, B.K. and Purton, J.A. (2000) Configurational lattice dynamics and hybrid Monte Carlo approaches to thermodynamic properties of solid solutions. *J. Molecular Structure – Thermochem.*, **506**, 45–53.

Bertram, U.C., Heine, V., Jones, I.L. and Price, G.D. (1990) Computer modeling of Al/Si ordering in sillimanite. *Phys. Chem. Miner.*, **17**, 326–33.

Balabin, A.I. and Sack, R.O. (2000) Thermodynamics of (Zn,Fe)S sphalerite: A CVM approach with large basis clusters. *Mineral. Mag.*, **64**, 923–44.

Bosenick, A., Dove, M.T., Warren, M.C. and Fisher, A. (1999) Local cation distribution of Diopside–Ca-Tschermak solid solutions: A computational and ^{29}Si MAS NMR spectroscopic study. *Eur. J. Mineral.*, **9**, 39.

Bosenick, A., Dove, M.T. and Geiger, C.A. (2000) Simulation studies of pyrope–grossular solid solutions. *Phys. Chem. Miner.*, **27**, 398–418.

Bosenick, A., Dove, M.T., Heine, V. and Geiger, C.A. (2001) Scaling of thermodynamic mixing properties in garnet solid solutions. *Phys. Chem. Miner.* (in press).

Carpenter, M.A., Powell, R., Salje, E.K.H. (1994) thermodynamics of nonconvergent cation ordering in minerals. 1. An alternative approach. *Amer. Mineral.*, **79**, 1053–67.

Carpenter, M.A. and Salje, E.K.H. (1994) Thermodynamics of nonconvergent cation ordering in minerals. 2. Spinels and the ortho-pyroxene solid-solution. *Amer. Mineral.*, **79**, 1068–83.

Clarke, L.J., Stich, I. and Payne, M.C. (1992) Large-scale ab initio total energy calculations on parallel computers. *Computer Phys. Comm.*, **72**, 14–28.

Craig, M.S., Warren, M.C., Dove, M.T., Gale, J.D., Sanchez-Portal, D., Ordejon, P., Soler, J.M. and

Artacho, E. (2001) Simulations of minerals using linear-scaling density functional theory based on atomic orbitals. *Phys. Chem. Miner.* (submitted).

Dove, M.T. (1999) Order/disorder phenomena in minerals: ordering phase transitions and solid solutions. Pp. 451–75 in: *Microscopic Processes in Minerals* (C.R.A. Catlow and K. Wright, editors). Kluwer, The Netherlands.

Dove, M.T. and Redfern, S.A.T. (1997) Lattice simulation studies of the ferroelastic phase transitions in $(Na,K)AlSi_3O_8$ and $(Sr,Ca)Al_2Si_2O_8$ feldspar solid solutions. *Amer. Mineral.*, **82**, 8–15.

Dove, M.T., Cool, T., Palmer, D.C., Putnis, A., Salje, E.K.H. and Winkler, B. (1993) On the role of Al/Si ordering in the cubic–tetragonal phase transition in leucite. *Amer. Mineral.*, **78**, 486–92.

Dove, M.T., Thayaparam, S., Heine, V. and Hammonds, K.D. (1996) The phenomenon of low Al/Si ordering temperatures in aluminosilicate framework structures. *Amer. Mineral.*, **81**, 349–62.

Dove, M.T., Bosenick, A., Myers, E.R., Warren, M.C. and Redfern, S.A.T. (2000) Modelling in relation to cation ordering. *Phase Trans.*, **71**, 205–26.

Gale, J.D. (1997) GULP: A computer program for the symmetry-adapted simulation of solids. *J. Chem. Soc.: Faraday Trans.*, **93**, 629–37.

Gasparik, T. (1984) Experimentally determined stability of clinopyroxene + garnet + corundum in the system CaO-MgO-Al_2O_3-SiO_2. *Amer. Mineral.*, **69**, 1025–35.

Hawthorne, F.C. (1997) Short range order in amphiboles: A bond valence approach. *Canad. Mineral.*, **35**, 210–16.

Lee, M.H., Cheng, C.F., Heine, V. and Klinowski, J. (1997) Distribution of tetrahedral and octahedral Al sites in gamma alumina. *Chem. Phys. Lett.*, **265**, 673–6.

McConnell, J.D.C., DeVita, A., Kenny, S.D. and Heine, V. (1997) Determination of the origin and magnitude of Al/Si ordering enthalpy in framework aluminosilicates from ab initio calculations. *Phys. Chem. Miner.*, **25**, 15–23.

Myers, E.R. (1999) *Al/Si ordering in silicate minerals*. PhD thesis, Univ. Cambridge, UK.

Myers, E.R., Heine, V. and Dove, M.T. (1998) Thermodynamics of Al/Al avoidance in the ordering of Al/Si tetrahedral framework structures. *Phys. Chem. Miner.*, **25**, 457–64.

Oberti, R., Ungaretti, L., Cannillo, E., Hawthorne, F.C. and Memmi, I. (1995) Temperature-dependent Al order–disorder in the tetrahedral double chain of *C*2/*m* amphiboles. *Eur. J. Mineral.*, **7**, 1049–63.

Okamura, F.P., Ghose, S. and Ohashi, H. (1974) Structure and crystal chemistry of Calcium Tschermak's pyroxene, $CaAlAlSiO_6$. *Amer. Mineral.*, **59**, 549–57.

Ordejón, P., Artacho, E. and Soler, J.M. (1996) Self-consistent order-*N* density-functional calculations for very large systems. *Phys. Rev. B*, **15**, 10441–4.

Palin, E.J., Dove, M.T., Redfern, S.A.T., Bosenick, A., Sainz-Diaz, C.I. and Warren, M.C. (2001) Computational study of tetrahedral Al-Si ordering in muscovite. *Phys. Chem. Miner.* (in press).

Patel, A., Price, G.D. and Mendelssohn, M.J. (1991) A computer-simulation approach to modeling the structure, thermodynamics and oxygen isotope equilibria of silicates. *Phys. Chem. Miner.*, **17**, 690–9.

Payne, M.C., Teter, M.P., Allan, D.C., Arias, T.A. and Joannopoulos, J.D. (1992) Iterative minimization techniques for abinitio total-energy calculations - molecular-dynamics and conjugate gradients. *Rev. Modern Phys.*, **64**, 1045–97.

Post, J.E. and Burnham, C.W. (1986) Ionic modeling of mineral structures and energies in the electron gas approximation: TiO_2 polymorphs, quartz, forsterite, diopside. *Amer. Mineral.*, **71**, 142–50.

Putnis, A. (1992) *Introduction to Mineral Sciences*. Cambridge University Press, Cambridge.

Redfern, S.A.T., Harrison, R.J., O'Neill, H.St.C. and Wood, D.R.R. (1999) Thermodynamics and kinetics of ordering in $MgAl_2O_4$ spinel from 1600°C from in situ neutron diffraction *Amer. Mineral.*, **84**, 299–310.

Sainz-Diaz, C.I., Hernandez-Laguna, A. and Dove, M.T. (2001) Modelling of dioctahedral 2:1 phyllosilicates by means of transferable empirical potentials. *Phys. Chem. Miner.* (in press).

Sanders, M.J., Leslie, M. and Catlow, C.R.A. (1984) Interatomic potentials for SiO_2. *J. Chem. Soc.: Chem. Comm.*, 1271–3.

Thayaparam, S., Dove, M.T. and Heine, V. (1994) A computer simulation study of Al/Si ordering in gehlenite and the paradox of the low transition temperature. *Phys. Chem. Miner.*, **21**, 110–6.

Thayaparam, S., Heine, V., Dove, M.T. and Hammonds, K.D. (1996) A computational study of Al/Si ordering in cordierite. *Phys. Chem. Miner.*, **23**, 127–39.

Vinograd, V.L. and Putnis, A. (1999) The description of Al, Si ordering in aluminosilicates using the cluster variation method. *Amer. Mineral.*, **84**, 311–24.

Vinograd, V.L., Putnis, A. and Kroll, H. (2001) Structural discontinuities in plagioclase and constraints on mixing properties of the low series: A computational study. *Mineral. Mag.*, **65**, 1–32.

Warren, M.C., Dove, M.T. and Redfern, S.A.T. (2000*a*) *Ab initio* simulations of cation ordering in oxides: application to spinel. *J. Phys.: Cond. Matter*, **12**, L43–8.

Warren, M.C., Dove, M.T. and Redfern, S.A.T. (2000*b*) Disordering of $MgAl_2O_4$ spinel from first principles. *Mineral. Mag.*, **64**, 311–7.

Warren, M.C., Dove, M.T., Myers, E.R., Bosenick, A., Palin, E.J., Sainz-Diaz, C.I., Guiton, B. and Redfern, S.A.T. (2001) Monte Carlo methods for the study of cation ordering in minerals. *Mineral. Mag.*, **65**, 221–47.

Winkler, B., Dove, M.T. and Leslie, M. (1991) Static lattice energy minimization and lattice dynamics calculations on minerals using three-body potentials. *Amer. Mineral.*, **76**, 313–31.

Wood, B.J., Kirkpatrick, R.J. and Montez, B. (1986) Order-disorder phenomena in $MgAl_2O_4$ spinel *Amer. Mineral.*, **71**, 999–1006.

[*Manuscript received 15 September 2000: revised 7 December 2000*]